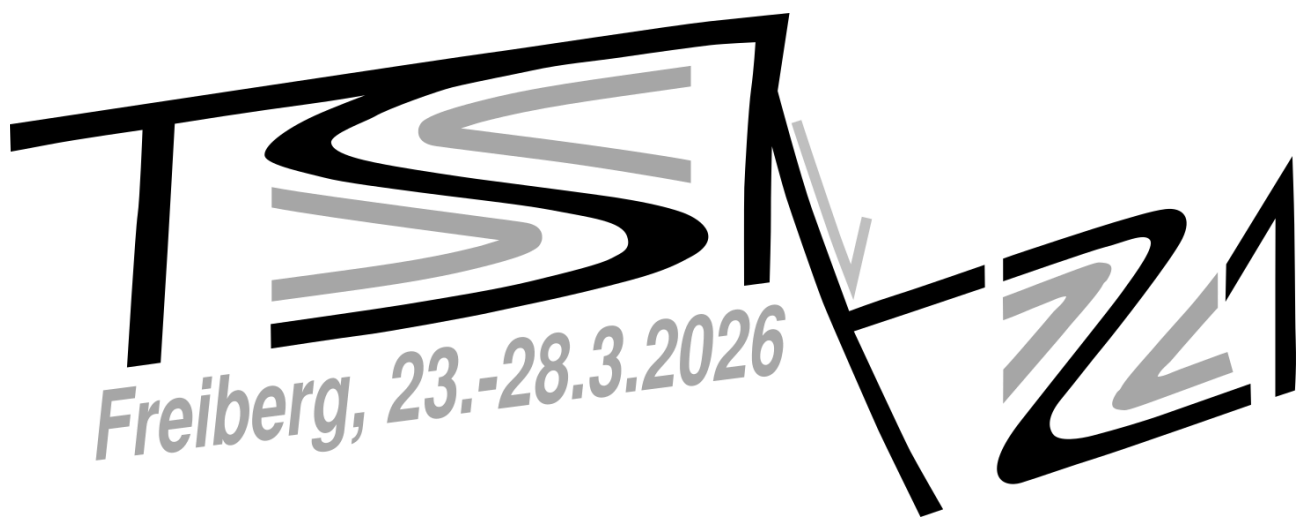


TSK Conference in Bergakademie Freiberg

Tektonik. Strukturgeologie. Kristallingeologie.



Talks

6

Folding of intrinsically anisotropic rocks and ice

Paul Bons and Yuan-Bang Hu

7

Glossar geologischer Brüche

Alena Broge, Berit Schwichtenberg, Jonas Kley, Bernd Leiss, and David C.P. Peacock

8

Diagenetic and detrital controls on the mechanical properties of sandstone

Yonghui Chen, Chaojie Cheng, Benjamin Busch, and Christoph Hilgers

9

Thrust imbrication and Late Cretaceous normal faulting in the western Austroalpine: The Arlui Fault and the Jaggl Mesozoic sediments (Ötztal Nappe, Vinschgau, Italy)

Nikolaus Froitzheim, Raphael Krag, Noah Schauen, and Jessika Ungerechts

10

The eastern termination of the Southern Steep Belt (Central Alps)

Simon L. Fuhrmann, Rüdiger Kilian and Thorsten Nagel

11

Microstructural Control of Fault Gouge Behaviour: Insights from Operando 4D

Synchrotron Microtomography

Nick Harpers, Florian Füsseis, and Eranga Jayawickrama

12

An extended extent of UHP metamorphism in the Erzgebirge wedge: some thoughts on its final structure and wedge-dome transition

Petr Jeřábek, Ondrej Lexa and Martin Racek

13

Stress- and time dependent permeability evolution of claystones and different sealing materials for CO₂ storage*Dorina Juhász, Benjamin Busch, Chaojie Cheng and Christoph Hilgers*

14

Tectonometamorphic architecture of the Erzgebirge

Martin Keseberg, Sebastian Weber, Ines Goerz, and Thorsten Nagel

15

Plate tectonic evidence for a Late Devonian lithospheric scale strike slip zone in Central Europe

Uwe Kroner

16

The microstructural record of oceanic core complex serpentinites - interaction of deformation and reaction

Rebecca Kühn, Luisa Schlickum, Marie C. Reichardt, Rüdiger Kilian, Luiz G. Morales, Andy Parsons, Barbara John, and Jeremy Deans

17

Predicting elastic anisotropy of foliated rocks based on laboratory measurements and macro-/microstructural observations (NW-Tauern Window, Austria)

Dustin Lang, Rebecca Kuehn, Rüdiger Kilian, and Michael Stipp

18

Limits of classical geothermal reservoir modelling in the Rhenohercynian Fold and Thrust Belt

Bernd Leiss and David C.P. Peacock

19

Brittle-ductile deformation of diopsidic clinopyroxene during incipient transformation of granulite to eclogite

Larissa Lenz, Sascha Zertani, Bernhard Grasemann, Roland Stalder, Luca Menegon, and Anna Rogowitz

20

Margins, Oceans, and Compression: What Controls Collision Architectures?

Iskander A. Muldashev and Thorsten J. Nagel

21

Interplay of metamorphism and deformation mechanisms in eclogite - Implications on transient mechanical behaviour at convergent settings.

Anna Rogowitz, Simon Schorn, and Benjamin Huet

22

Variscan tectonics of the Elbe Zone – Pervasive strike-slip overprint of a pre-existing accretionary complex <i>Lea Schulze and Uwe Kroner</i>	23
Small Inclusions, Big Implications: Tracing the Polymetamorphic Variscan Evolution of the Southern Bohemian Massif <i>Dominik Sorger, Christoph A. Hauzenberger, Fritz Finger, Manfred Linner, Christoph Iglseder, Etienne Skrzypek, Simon Schorn, and David Günzler</i>	24
Intraplate paleoseismicity in low seismic settings of Central Europe (Germany) <i>Vanessa Steinritz and Klaus Reicherter</i>	25
Birth, Life and Fate of a Hadal Basin in the Japan Trench <i>Michael Stipp et al.</i>	26
Intrusive and extrusive evolution of two Late Carboniferous calderas in the NW Bohemian Massif <i>Filip Tomek, Petr Vitouš, and Irena Olšanská</i>	27
A virtual KTB (Kontinentale TiefBohrung): The ultimate benchmark for apatite fission track annealing? <i>Florian Trilsch, Raymond Jonckheere, and Thorsten Nagel</i>	28
Late Carboniferous geomagnetic field events captured by Altenberg–Teplice Caldera, Bohemian Massif <i>Petr Vitouš, Michael S. Petronis, Marine S. Foucher, and Filip Tomek</i>	29
A juvenile arc terrane in the Mid-German Crystalline Zone – constraints from zircon U-Pb-Hf isotope data and implications for pre- to syn-Variscan evolution <i>Armin Zeh, Marius Beck, Matthias Hinderer, Henri P. Meinaß, and Axel Gerdes</i>	30
Posters	31
Experimental and microstructural study on the effect of second phase particles on compaction mechanisms of halite <i>Marleen Bodenstein, Rüdiger Kilian, André Eschenröder, Florian Fritz, Maximilian Köhne, and Michael Stipp</i>	32
Tectono-Structural Evolution of the Pre-Devonian Basement, Inner Billefjorden, Svalbard <i>Muriel Bühlhoff, Aleksandra Smyrak-Sikora, Kim Senger, and Hannah Pomella</i>	33
Development of a polyphase basement: Ograzhden Unit, SW Bulgaria <i>Alex Jensen, Jan Pleuger, Xin Zhong, Elis Hoffmann, Stoyan Georgiev, and Jessica Stammeier</i>	34
Previously unrecognized high-pressure metamorphism in the Eastern Erzgebirge. <i>Martin Keseberg, Tristan Lange, Tim Koark, Till Burock, and Thorsten Nagel</i>	35
In-Sequence Thrusting and Triangle Zone Development in the External Dinarides: Constraints from 2D Kinematic Forward Modelling of a cross section around the Drežnica Canyon, Bosnia and Herzegovina <i>Marah Kieckbusch, Philipp Balling, and Kamil Ustaszewski</i>	36
G.O.Joe: A new online tool for LA-ICP-MS data reduction <i>Joachim Krause, Florian Altenberger, Thomas Auer, Alexander Auer, and Jasper Berndt</i>	37
The eastern Ruhla Crystalline Complex: Evidence for multi-directional deformation <i>Georg Löwe and Peter Hallas</i>	38

Trace element distribution in sulfides of the Kupferschiefer-Type mineralization, Röhrigschacht Wettelrode (Saxony-Anhalt) <i>Christian Lohmann, Nico Kropp, Ralf Halama, Harilaos Tsikos, and Michael Stipp</i>	39
Exhumation through Vertical Extrusion: A Modeling Study of the Rhodope Metamorphic Complex <i>Iskander A. Muldashev and Thorsten J. Nagel</i>	40
Seismic velocity profiles, petrological velocity modeling and the architecture of the crust in Bulgaria <i>Thorsten Nagel, Gergana Georgieva, and Christian Schiffer</i>	41
Operando 4D synchrotron tomography reveals transport-controlled multiphase dolomitization in natural carbonate rock <i>Arthur Ng, Nick Harpers, Andrew King, and Florian Fuisseis</i>	42
Influence of initial grain size on quartz deformation and static recovery <i>Malte Ortmanns, Petar Pongrac, Petr Jerabek, Sebastian Cionoiu, Jean Furstoss, Yuval Boneh, and Lucie Tajcmanova</i>	43
Ar-Ar geochronology I - Applications, limitations, developments and future <i>Jörg A. Pfänder, Blanka Sperner, and Thorsten Nagel</i>	44
Magmatic plumbing systems and their role in continental breakup - an example from Messum, Namibia <i>Jörg A. Pfänder, Philipp Holaschke, Joachim Krause, Andreas Klügel, Thorsten Nagel, Stefan Jung, and Carsten Münker</i>	45
Poly-metamorphic evolution of a slice of the Briançonnais terrane: structural and petrographic evidence from the Tambo Nappe (Central Alps) <i>Enrico Pigazzi, Francesco Arrigoni, Leo J. Millonig, Filippo L. Schenker, Axel Gerdes, Paola Tartarotti, and Lucie Tajčmanová</i>	46
Do quartz-in-garnet Raman spectroscopic data and garnet fabrics reveal a fluid infiltration event in the south of the Adula nappe? <i>Jan Pleuger, Xin Zhong, Olga Brunsmann, Kristina G. Dunkel, Marisa Germer, Vincent Könnemann, Victoria Kohn, Luca Menegon, Guyu Peng, Alexandra Pohl, Julien Reynes, and Timm John</i>	47
Microanalysis of Shock Experiments on K-Feldspar <i>Michael H. Poelchau, Dominic Wölki, and Thomas Kenkmann</i>	48
The Paku Tin Deposit: A Deformed Greisen Mineralization? <i>Nimatul Azizah Raharjanti, Joachim Krause, Arifudin Idrus, Ernowo, Wahyu Vian Pratama, and Jens Gutzmer</i>	49
Serpentinization of orthopyroxene in oceanic serpentinites <i>Marie C. Reichardt and Rebecca Kühn</i>	50
Microstructural evidence of tectonic overpressure. <i>Anna Rogowitz, Philippe Goncalves, Bernhard Grasemann, Zhaoliang Hou, and A. Hugh N. Rice</i>	51
Spinel-bearing cumulate dunite in garnet-bearing ultramafic rocks of Zöblitz (Erzgebirge) - Implications for the pre-subduction evolution of mantle-derived ultramafic rocks in the Erzgebirge UHP terrane <i>Kilean Rohr, Joachim Krause, Jörg A. Pfänder, Sabine Gilbricht, and Stefan Jung</i>	52
The Miocene tectonic evolution of the western Tauern Window (European Alps): A spatial-temporal restoration	

<i>Julia Rudmann, David C. Tanner, Hannah Pomella, Christian Brandes, Paul Eizenhöfer, and Michael Stipp</i>	53
(Micro-) tectonics of tin bearing metasedimentary rocks of the Erzgebirge <i>Owishi Sarkar, Ida Hemplen, Uwe Kroner, Claus Legler, and Rolf L. Romer</i>	54
Magnetite microstructure in oceanic serpentinites <i>Luisa Schlickum, Rüdiger Kilian, and Rebecca Kühn</i>	55
Triaxial testing on rock salt in the context of hydrogen storage in caverns <i>Friedrich Schlosser, Florian Fritz, Rüdiger Kilian, André Eschenröder, and Michael Stipp</i>	56
Structural field observations of the Rechnitz Window (Austria, Hungary) <i>Bettine Sievers, Greta Siewert, Amina Redzematovic, Paola Manzotti, László Fodor, Benjamin Huet, and Jan Pleuger</i>	57
Peak temperatures of metasediments from the Rechnitz Window Group (Austria, Hungary) determined by Raman spectroscopy on carbonaceous matter <i>Greta Siewert, Bettine Sievers, Amina Redzematovic, Paola Manzotti, Laszlo Fodor, Benjamin Huet, and Jan Pleuger</i>	58
Progressive fabric development in crustal scale shear zone: insights from integrated AMS, PGR, and SPO analyses <i>Swagata Singha, Tridib Kumar Mondal, Susanta Kumar Samanta, and Subhabrata Das</i>	59
Ar-Ar geochronology II - Deciphering the code: Interpretation of complex Ar isotope data <i>Blanka Sperner and Jörg A. Pfänder</i>	60
Marine Mn redox evolution tracks the Great Oxidation Event <i>Harilaos Tsikos, Jarryd Labuschagne, Petros Koutsovitis, and Paul RD Mason</i>	61
An isoclinal and boudinaged synformal anticline in the Reckner Nappe of the Tarntal Mesozoic (Lower Austroalpine), Eastern Alps <i>Kamil Ustaszewski and Philipp Balling</i>	62
Two types of serpentinite from the Saxon Granulite Massif (Bohemian Massif, Germany) <i>Sebastian Weber, Martin Keseberg, and Thorsten Nagel</i>	63
Multistage vein fracturing and gold mineralization: insights from the Linglong orogenic gold deposit, China <i>Peng-Cong Zhang, Anna Rogowitz, Hao-Cheng Yu, Clifford Patten, and Kun-Feng Qiu</i>	64

Talks

Folding of intrinsically anisotropic rocks and ice

Paul Bons¹ and Yuan-Bang Hu²

¹ Department for Geosciences, Tübingen University, paul.bons@uni-tuebingen.de

² Center for High Pressure Science and Technology Advanced Research, Beijing 100193, China

A cleavage formed by alignment of micas or a strong crystallographic orientation gives a rock an intrinsic anisotropy. Classical Biot-type fold theory - with layer thickness controlling the length scale - does not apply because anisotropy has no length scale to determine fold wavelengths. Analyses of the power spectra of folded biotite schist and numerical simulations with Elle-FFT show that the folds in intrinsically anisotropic rocks are self-similar (Fig. 1): they have no characteristic wavelength, in contrast to Biot-type buckle folds (Bons et al. 2025). This means that self-similar folds detected in polar ice sheets also formed due to shortening parallel to the strong CPO of the ice. Recognising the major impact of anisotropy on folds, this talk also explores other consequences, from porphyroclast geometries, shear localisation, to sutures in subduction systems.

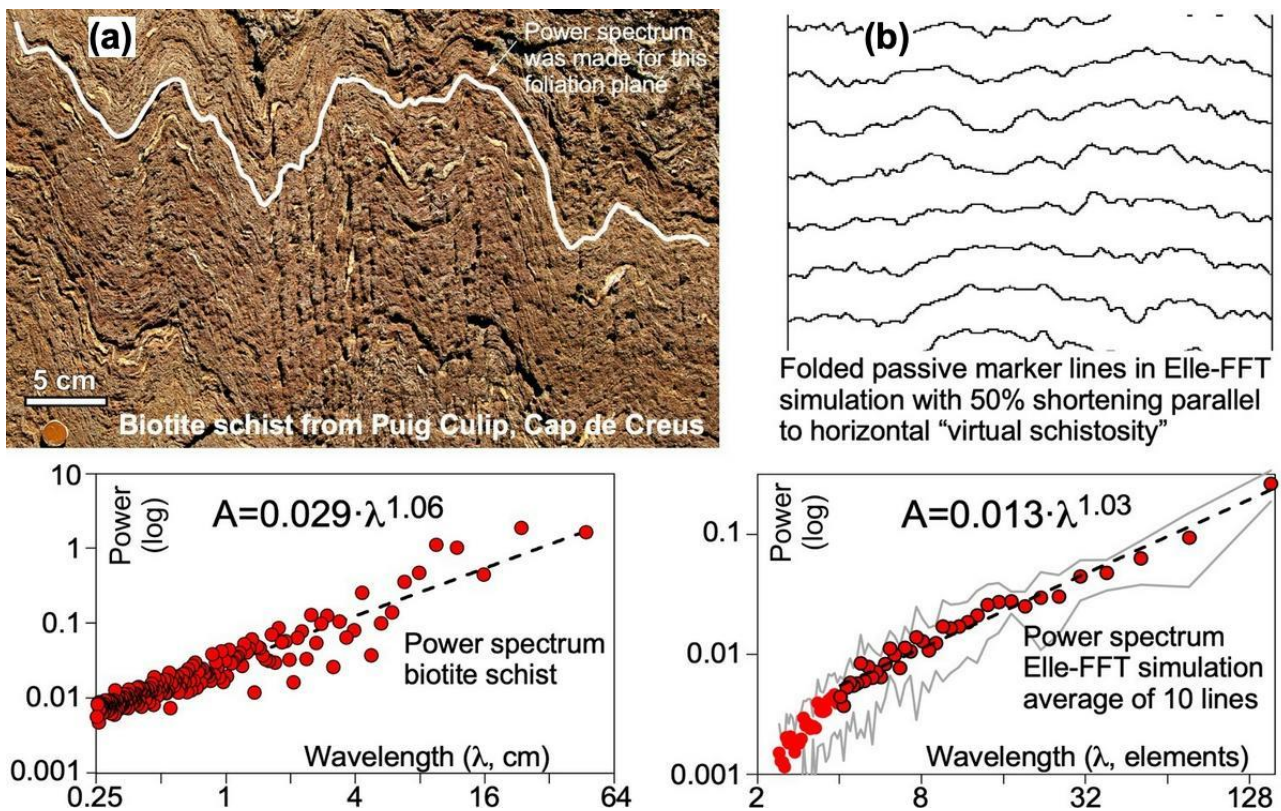


Figure 1: Natural (a) and numerical (b) folds in strongly anisotropic material, with associated power-spectra shown below. The power-law exponent of about one indicates the folds are self-similar.

References

Bons, P.D., Hu, Y., Llorens, M.-G., Franke, S., Stoll, N., Weikusat, I., Westhoff, J., Zhang, Y. 2025. Folding due to anisotropy in ice, from drill core-scale cloudy bands to km-scale internal reflection horizons. *The Cryosphere* 19, 5095–5109.

Doi: <https://tc.copernicus.org/articles/19/5095/2025/>.

Glossar geologischer Brüche

Alena Broge¹, Berit Schwichtenberg², Jonas Kley¹, Bernd Leiss¹, and David C.P. Peacock¹

¹*Geowissenschaftliches Zentrum der Universität Göttingen, Strukturgeologie & Geothermik, Goldschmidtstraße 3, 37077 Göttingen, Deutschland*

²*Universität Bern, Institut für Geologie, Baltzerstrasse 1+3, 3012 Bern, Schweiz*

Aktuelle Forschung im Feld der Strukturgeologie wird überwiegend in englischer Sprache verfasst. Dies ist oft vorteilhaft, weil es die Kommunikation von Wissenschaftlern aus aller Welt auf dem gleichen Feld ermöglicht. Jedoch führt die Vielzahl der, teils neu eingeführten, Begriffe selbst bei Muttersprachlern häufig zu Verwirrung im Gebrauch korrekter Terminologie. Zudem gibt es Situationen, in denen die Verwendung deutscher Fachbegriffe unabdingbar ist, wie etwa in Berichten und Gutachten, für die deutsches Recht eine Rolle spielt. Prominente Beispiele hierfür sind die Standortauswahl für Endlager radiogener Stoffe oder die Erschließung geothermischer Reservoirs.

Mit dem Glossar liefern wir deutsche Übersetzungen von Begriffen, die im Englischen zur Beschreibung spröder Strukturen gebräuchlich sind. Es ist zu beachten, dass wir nur eine Momentaufnahme bzw. einen Rückblick auf die Bedeutung dieser Begriffe liefern können, da sich die Sprache im Laufe der Zeit weiterentwickelt und neue Begriffe entstehen oder sich die Bedeutung bestehender Begriffe verändert. Wir hoffen jedoch, dass diese Übersetzungen und ihre Erläuterungen für deutschsprachige Leser nützlich sind und das internationale Verständnis und die Zusammenarbeit unterstützen. Angesichts der zunehmenden Nutzung von Künstlicher Intelligenz (KI) zur Textproduktion und Übersetzung gewinnt die Verfügbarkeit möglichst präziser, kuratierter „Lerndaten“ besondere Bedeutung, um die unkontrollierte Etablierung mehrdeutiger oder fachlich ungenauer Bezeichnungen zu vermeiden.

Wir skizzieren Auswahl- und Abgrenzungskriterien für Neuübersetzungen, den Umgang mit konkurrierenden deutschen Übersetzungen und etablierten Anglizismen sowie den Einsatz von KI-gestützten Werkzeugen zur sprachlichen Überarbeitung. Abschließend diskutieren wir, welche Ansätze sich als besonders hilfreich erwiesen haben und wo konzeptionelle oder terminologische Probleme aufgetreten sind.

References

Broge, A.; Schwichtenberg, B.; Kley, J.; Leiss, B.; Peacock, D. C. P. (2025): From faults to fractures – a German glossary based on English terms. In: ZDGG 176, S. 301–358. DOI: 10.1127/zdgg/2025/0489.

Diagenetic and detrital controls on the mechanical properties of sandstone

Yonghui Chen¹, Chaojie Cheng¹, Benjamin Busch¹, and Christoph Hilgers¹

¹ *Structural Geology & Tectonics, Institute of Applied Geosciences, Karlsruhe Institute of Technology (KIT), Adenauerring 20a, 76131 Karlsruhe, Germany*

Accurate prediction of sandstone mechanical properties is essential for geotechnical engineering, reservoir management, and subsurface energy storage. The diagenetic processes, particularly compaction and cementation, not only control the porosity and permeability of sandstones but also strongly affect their mechanical strength. Although uniaxial compressive strength (UCS) generally increases with decreasing porosity, the extent to which diagenetic cementation and associated fracture mechanisms modulate this relationship has not been systematically quantified.

In this study, we investigate how diagenetic alterations, including porosity reduction and cementation type, govern the UCS of sandstones collected from Lower Triassic Buntsandstein outcrops at the Upper Rhine Graben shoulder in south-western Germany. Cylindrical samples drilled mainly perpendicular to bedding exhibit porosities of 4–25% and permeabilities from 0.001 to 10000 mD, reflecting varying diagenetic intensities. UCS values range from 17 to 179 MPa, with corresponding Young's modulus of 8–50 GPa and P-wave velocities between 2122 and 4132 m/s. The results demonstrate that high-porosity samples with low cement content predominantly fail through fracture coalescence along pre-existing defects, whereas low-porosity samples with abundant cement exhibit grain-scale fracture propagation. Additionally, we detected two main categories exhibiting different degrees of strength enhancement with porosity reduction, namely brittle-cement (e.g., quartz, feldspar) dominance and ductile-cement (e.g., clay minerals) dominance. In a low-porosity regime (<15%), brittle cementation produces a markedly stronger increase in UCS than ductile cementation, whereas at high porosity, cementation exerts minimal control on failure mechanisms. These findings reveal that sandstone strength is not governed solely by porosity magnitude, but by the coupled effects of cement type, porosity evolution, and fracture processes. This mechanistic framework enables an improved strength prediction for porous sandstone reservoirs and subsurface engineering applications.

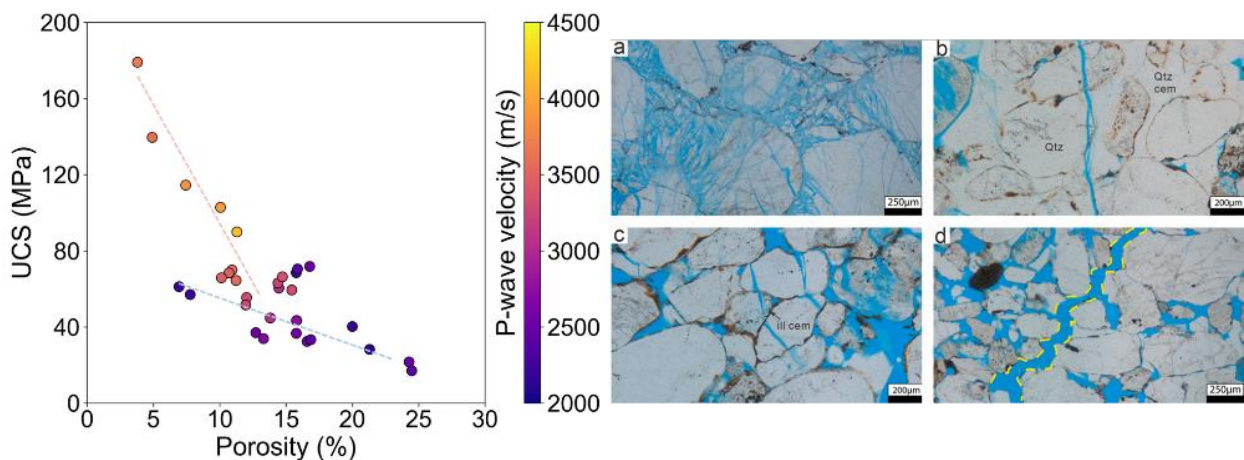


Figure 1. Relationships between porosity, UCS, P-wave velocity, and microstructures in Sandstone.

Thrust imbrication and Late Cretaceous normal faulting in the western Austroalpine: The Arlui Fault and the Jaggl Mesozoic sediments (Ötztal Nappe, Vinschgau, Italy)

Nikolaus Froitzheim, Raphael Krag, Noah Schauen, and Jessika Ungerechts

Institut für Geowissenschaften, Universität Bonn; niko.froitzheim@uni-bonn.de

Jaggl is a mountain in the Upper Vinschgau, built up of Mesozoic sedimentary rocks and surrounded by crystalline basement rocks of the Ötztal Nappe. It is debated whether the sediments represent the cover of the Ötztal Nappe (“cover hypothesis”) or a tectonic window into a deeper nappe (“window hypothesis”). A key role is played by the steeply southeast-dipping Arlui Fault along which the Jaggl Mesozoic rocks to the Southeast are in contact with Ötztal basement rocks to the Northwest. In the “window hypothesis”, the displacement along the Arlui Fault should be southeast-side-up, whereas in the “cover hypothesis”, it should be southeast-side-down. Our study of ductile (lower greenschist facies) to brittle fault rocks along the Arlui Fault yielded exclusively evidence for southeast-side-down, i.e., normal faulting. In addition, we identified the prolongation of the Arlui Fault towards northeast, represented by a top-southeast, greenschist-facies mylonite zone within the amphibolite-facies Ötztal basement. The Arlui Normal Fault belongs to the system of normal faults that overprinted the Austroalpine nappe stack during the Late Cretaceous, the Jaggl rocks are a downthrown part of the cover of the Ötztal Nappe, and the “Jaggl Window” does not exist.

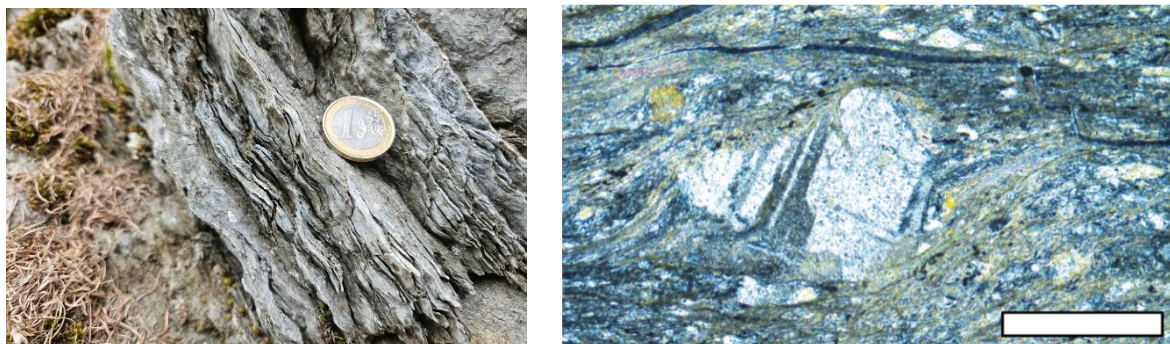


Figure 1. Top-Southeast (dextral) shear-sense criteria in mylonitized Permian volcanics from the footwall of the Arlui Fault. Left: shear bands; right: sigma-type porphyroblast of plagioclase. Southeast is to the right in both images; scale bar is 0.5 mm.

The eastern termination of the Southern Steep Belt (Central Alps)

Simon L. Fuhrmann¹, Rüdiger Kilian², and Thorsten Nagel¹

¹ *TU Bergakademie Freiberg, Institute of Geology, Germany, kontakt@simon-fuhrmann.de*

² *Martin-Luther-University Halle-Wittenberg*

The Southern Steep Belt (SSB) is an E-W-striking, north-block-up mylonite zone that juxtaposes high-grade metamorphic Europe-derived basement nappes and the unmetamorphic Southern Alps. At its eastern end in the upper Valle dei Ratti, this mylonite zone apparently terminates at the calc-alkaline Bergell pluton (BP), where a large antiform at the base of the BP translates the intrusive rocks together with the underlying gneisses of the Gruf complex (GC) into the SSB. Nevertheless, the relationship between the SSB and the units farther north, such as the GC and the Adula nappe, remains disputed.

We present a new geological map of this critical area. The presence of an alternating sequence of Bt-rich gneisses and schists adjacent to more leucocratic gneisses, as well as metasedimentary and meta-ultramafic rocks, clearly indicates the existence of a single basement unit beneath the BP. This contradicts previous maps, which assigned different tectonic units to the two limbs of the antiform (Berger, 1996). Stretching lineations and fold axes consistently plunge eastward. Structural, microstructural, and EBSD data indicate upper-unit-to-the-east shearing, which transitions into north-block-up, left-lateral shearing within the SSB. We propose that the mylonitic shear zone of the SSB is folded together with the base of the BP and continues farther north into a right-lateral, south-block-up shear zone at the northern border of the Gruf complex (Galli et al., 2013). Therefore, top-to-the-east shearing beneath the BP would exhume the entire Lepontine dome, not just the Gruf complex. This model would explain the metamorphic gap on the northern and southern sides of the Gruf complex as well as the absence of the SSB east of the BP.

References

- Berger, A., 1996. Geological-tectonic map of the Bergell pluton: *Schweizerische Mineralogische und Petrographische Mitteilungen*, **76**.
Galli, A., Le Bayon, B., Schmidt, M.W., Burg, J.-P. and Reusser, E., 2013. Tectonometamorphic history of the Gruf complex (Central Alps): exhumation of a granulite–migmatite complex with the Bergell pluton: *Swiss Journal of Geosciences*, **106**, p. 33–62, doi: 10.1007/s00015-013-0120-1.

Microstructural Control of Fault Gouge Behaviour: Insights from Operando 4D Synchrotron Microtomography

Nick Harpers¹, Florian Füsseis¹, and Eranga Jayawickrama¹

¹RWTH Aachen University, Germany n.harpers@asg.rwth-aachen.de

Fault zones are intrinsically heterogeneous, multiscale systems whose mechanical and hydraulic behaviour emerges from tightly coupled thermal-hydraulic-mechanical-chemical (THMC) processes. In the context of subsurface energy applications – deep geothermal exploitation, CO₂- and H₂-storage or radioactive waste storage – faults may act either as preferential flow conduits or as hydraulic barriers, while simultaneously representing potential nucleation sites for induced seismicity. Their macroscopic response is governed by evolving microstructure, mineral reactions, pore-fluid redistribution, and stress transfer. However, isolating and quantifying these dynamic feedbacks under controlled boundary conditions remains experimentally challenging, particularly during ongoing deformation.

To address this limitation, we employ operando 4D synchrotron microtomography combined with our X-ray transparent, heatable triaxial deformation apparatus Heitt Mjölñir. The system integrates a newly developed direct-shear inset that converts axial displacement into controlled shear strain within thin gouge layers, enabling deformation geometries representative of natural fault cores. Continuous shearing is imaged at high temporal resolution under in situ pressure–temperature conditions, linking evolving microstructures to simultaneously recorded macroscopic parameters such as shear stress, normal stress, and displacement. This configuration allows bidirectional interrogation: structural evolution as a function of imposed boundary conditions, and mechanical response as a function of emergent internal architecture.

This approach provides quantitative access to transient structural states that are otherwise inaccessible in post-mortem analyses. It enables time-resolved tracking of strain localisation, compaction/dilation cycles, and reaction-induced fabric reorganisation, thereby constraining how microstructural reconfiguration modulates frictional strength and hydraulic connectivity. By resolving these feedbacks during active deformation, the method establishes a direct bridge between THMC process evolution and fault stability, offering experimentally grounded constraints for constitutive descriptions of deforming gouges and improved assessment of seismic and hydraulic risks in engineered subsurface systems.

An extended extent of UHP metamorphism in the Erzgebirge wedge: some thoughts on its final structure and wedge-dome transition

Petr Jeřábek¹, Ondrej Lexa¹, and Martin Ráček¹

¹ *Institute of Petrology and Structural Geology, Faculty of Science, Charles University, Prague* jerabek.petr@natur.cuni.cz

Our recent discoveries of coesite-bearing rocks in the Eger and Erzgebirge crystalline complexes (Závada et al. 2021; Lexa et al. 2026; Ráček et al. 2026) indicate more widespread occurrence of Ultrahigh-Pressure (UHP) metamorphism than previously thought. In the Eger complex, coesite occurs not only in felsic granulite as previously reported by Kotková et al. (2011) but also in granofels and quartzo-feldspathic ultramylonite. Identical assemblage of rocks and the coesite-bearing ultramylonite was discovered also in the vicinity of the Přísečnice dam in the Erzgebirge suggesting the affinity of the two complexes. This is consistent with the previous findings of diamond-bearing gneiss near the Saldenbach reservoir in the Erzgebirge and near Stráž nad Ohří in the Eger complex (Nasdala and Massonne, 2000; Kotková et al. 2011). Our recent discovery of jadeite- and coesite-bearing gneiss west of Chomutov (Lexa et al. 2026) complements the currently known extent of UHP rocks in the Erzgebirge. Spatial distribution of the UHP rocks is semi-concentric to the structurally lowermost unit of the Erzgebirge complex, the so called Kateřina-Reitzenhain unit. This unit shows relatively high temperature and medium pressure orthogneiss fabric recently dated by U-Pb monazite to ~332-330 Ma which contrasts with microstructures and ages documented in the surrounding units (Kryl et al. 2021). Indeed, our compilation of geochronological data indicate that the main stage of the Erzgebirge wedge formation occurred between ~360-338 Ma while its final structure was completed between ~335-328 Ma (Jouvent et al. 2023 and references therein). In contrast to the previous interpretations, we propose that deformation and metamorphism in the Kateřina-Reitzenhain unit is associated with the late evolution of the Erzgebirge, possibly reflecting its southward underthrusting below the Erzgebirge wedge, and thus marking the wedge to dome transition of the entire complex.

References

- Jouvent, M., Peřestý, V., Jeřábek, P., Lexa, O., Kylander-Clark, A.R.C., 2023. *Tectonics* 42, e2022TC007626.
 Kotková, J., O'Brien, P.J., Ziemann, M.A., 2011. *Geology* 39, 667–670.
 Kryl, J., Jeřábek, P., Lexa, O., 2021. *Tectonophysics* 820, 229096.
 Lexa, O., Ráček, M., Jeřábek, P., Paddon, B., 2026. *Journal of Metamorphic Geology*, in press.
 Nasdala, L., Massonne, H.-J., 2000. *European Journal of Mineralogy* 12, 495–498.
 Ráček, M., et al. *American Mineralogist*, in press.
 Závada, P. et al. *Chemical Geology* 559, 119919.

Stress- and time dependent permeability evolution of claystones and different sealing materials for CO₂ storage

Dorina Juhász¹, Benjamin Busch¹, Chaojie Cheng¹, and Christoph Hilgers¹

¹ *Karlsruhe Institute of Technology, Institute of Applied Geosciences – Structural Geology and Tectonics, 76131 Karlsruhe, Adenauerring 20a, Germany*

Carbon Capture and Storage (CCS) is a promising approach that has been increasingly utilized for reducing atmospheric carbon dioxide (CO₂) levels. The long-term security of CO₂ sequestration depends on the integrity of overlying sealing units, while the transmissive properties of multi-barrier sealing systems remain to be further elaborated. This study investigates the permeability of claystones and compares them with other low-permeability lithologies (evaporites, tight sandstones, and tight limestones, 1×10^{-17} - 1×10^{-21} m² at 30 MPa) as well as casing cements (1×10^{-16} - 1×10^{-22} m² at 30 MPa) under CO₂ storage conditions. Permeability was measured using helium gas and, for selected samples, with CO₂. Klinkenberg-corrected permeability was assessed under confining pressures of 10 – 30 MPa, and pressure sensitivity coefficients (γ -values) were determined. Time-dependent effects were evaluated by maintaining samples at 30 MPa (approximately 2 km depth) confining pressure for 5-8 days. Results indicate that claystones reduce permeability by approximately one order of magnitude after 3-5 days, while casing cements decrease permeability by two orders of magnitude in 3 days. These findings highlight the necessity of allowing caprock samples to equilibrate under targeted effective stresses for at least three days to obtain reliable permeability measurements. Furthermore, permeability varies distinctly across lithotypes (shales, evaporites, tight sandstones, and tight limestones), spanning 2 to 6 orders of magnitude at low confining stresses, necessitating the site- and lithotype-specific assessment of sealing unit permeability.

Tectonometamorphic architecture of the Erzgebirge

Martin Keseberg¹, Sebastian Weber², Ines Goerz², and Thorsten Nagel¹

¹ *TU Bergakademie Freiberg, Martin.Keseberg@geo.tu-freiberg.de*

² *LfULG Sachsen*

We present a revised scheme for the tectono-metamorphic architecture of the Erzgebirge, based on our study of the distribution of high-pressure metamorphism and our compilation of three large-scale cross-sections. Sharp contrasts in protoliths correlate with changes in metamorphic evolution and we infer a nappe stack that consists from bottom to top of the following units: (1) a Lower Gneiss Unit (LGU) comprising gneisses with both Proterozoic and Ordovician protoliths, which experienced amphibolite-facies peak metamorphism. (2) An Upper Gneiss Unit (UGU) characterized by eclogite-facies peak metamorphism. While Proterozoic protoliths predominate, we also define subunits with Ordovician protoliths, which partly experienced ultra-high-pressure conditions. In contrast to previous studies, we find eclogites throughout the UGU indicating a more coherent unit. (3) A Mica Schist Unit (MSU) that likewise consists of two subunits: the larger subunit, the MSU *sensu stricto*, is made of Ordovician metasediments and rare amphibolite and experienced only blueschist- to amphibolite-facies peak conditions. The second, smaller subunit is exposed as an internal nappe and consists of HP-gneisses and eclogites from various Ordovician protoliths. While these lithologies are similar to those found in the subunits of the UGU, a lack of data in the latter makes it difficult to confirm a relationship. Nevertheless, we follow existing schemes that propose an original tectonic position on top of MSU *sensu stricto*. We interpret the Erzgebirge as a stack of nappes that was assembled after peak-pressure conditions were reached in most units. While postnappe deformation might have complicated the structural record, we conclude that the LGU, UGU and MSU occupy their original, progressively higher tectonic positions in the stack.

Plate tectonic evidence for a Late Devonian lithospheric scale strike slip zone in Central Europe

Uwe Kroner

Department of Geology, TU Bergakademie Freiberg, B.-v.-Cotta-Strasse 2, D-09599 Freiberg, Germany

Late Devonian mantle-derived rocks are common in the internal zones of the Central European Variscides. These occurrences are explained by various models in different ways, such as for example: i) back arc setting due to the subduction of Paleo-Tethys [1], ii) relict of a Devonian-Carboniferous ocean [2]. There is, however, ample evidence of coeval juvenile magmatism on the Peri-Gondwana continental shelf. Here, I discuss a ca. 1000 km, SW–NE-oriented, narrow magmatic belt spanning from the Sudetes to the Western Alps. Ophiolitic sequences occur, for example, in the Chamrousse Complex (French Western Alps), the Vosges Mountains (France), and Saxo-Thuringia (Germany). The entire belt is characterised by bimodal magmatism and marine sedimentation. The presence of isolated islands is indicated by conglomerates containing debris from late Devonian magmatic rocks. Moreover, the proximity of deep and shallow marine environments further underlines the complex architecture. I explain this complexity by the former presence of a lithospheric-scale strike-slip zone during SW-NE directed plate convergence [3].

The proposed plate tectonic scenario is as follows: Late Devonian opening of Paleo-Tethys (~370 Ma) occurred south of the Variscan plate boundary zone and resulted in plate tectonic reorganisation during ongoing convergence of Gondwana and Laurussia. Accretionary tectonics occurred at this time in the future French Massif Central, as well as in the future Bohemian Massif. The newly formed, SW-NE striking belt acted as a lithospheric-scale transfer zone, sustaining strain compatibility between the two collisional domains. Transtensional areas are characterised by juvenile magmatism, whereas transpressional domains are characterised by uplift and erosion. Early Carboniferous crustal stacking subsequently occurred parallel to the strike of the belt, as evidenced by NE-SW stretching lineations. Finally, late Variscan transpressional tectonics, affecting the exhumed low- to medium-grade metamorphic/metasedimentary lithologies, occurred in a NW-SE direction. Although this zone was significantly modified by subsequent stages of the Variscan orogeny, the general structure of this intra-continental, lithospheric-scale transfer zone can still be seen.

References:

- [1] Skrzypek, E. et al., 2011. The significance of Late Devonian ophiolites in the Variscan orogen: a record from the Vosges Klippen Belt. *International Journal of Earth Sciences*, 1-22.
- [2] Gunia, M., et al. 2025. The Chamrousse Ophiolite (Western Alps, France): Relict of a Devonian-Carboniferous Ocean. *Terra Nova*, 1-6.
- [3] Kroner, U., et al. 2022. Paleozoic orogenies and relative plate motions at the sutures of the Iapetus-Rheic Ocean. *New Developments in the Appalachian-Caledonian-Variscan Orogen*, 1-23.

The microstructural record of oceanic core complex serpentinites - interaction of deformation and reaction

Rebecca Kühn¹, Luisa Schlickum¹, Marie C. Reichardt¹, Rüdiger Kilian¹, Luiz G. Morales²; Andy Parsons³, Barbara John⁴, and Jeremy Deans⁵

¹ *MLU Halle, rebecca.kuehn@geo.uni-halle.de*

² *ETH Zurich*

³ *University of Plymouth*

⁴ *University of Wyoming*

⁵ *University of Southern Mississippi*

At mid-ocean ridges new oceanic crust is formed from adiabatic melting. When the melt production is not high enough to keep up with the spreading rate, the spreading process is accommodated by detachment faulting. The detachment fault footwall exposed to the seafloor consists of ultramafic and mafic rocks. The exhumed ultramafics are most often serpentinitized, leaving the question open whether fluid availability and serpentinitization allow for faulting or whether the faulting allows for serpentinitization.

The Atlantis Massif at 30° N, is such a detachment fault footwall, a so called oceanic core complex. IODP expedition 399 drilled a 1.2 km deep hole into the Atlantis Massif, recovering ultramafic rocks which are 40-100% serpentinitized, as well as mafic rocks. These rocks provide a unique insight into the interaction of serpentinitization and tectonic processes. Using a combined approach of microstructural methods such as optical and electron microscopy, EBSD, synchrotron diffraction, as well as μ XRF and EDS mappings, we explore which processes dominate at which stage during the formation and exhumation of the Atlantis Massif.

The pre-serpentinitization microstructure of incompletely serpentinitized rocks is reconstructed. Peridotite deformation, most likely due to detachment faulting at greater depths, is only sparsely documented by mylonitic grain size reduction.

Subsequent serpentinitization overprints these early structures. Besides typical mesh microstructures, serpentinites often show a parallel alignment of elongate magnetite aggregates with serpentine basal planes aligned parallel to the magnetite aggregate long axis, resulting in a crystallographic preferred orientation. In certain depths of the drill core, microfaulting of the serpentinite is ubiquitous.

Whether these observations relate to conditions during serpentinitization or deformation of the serpentinites will be discussed.

Predicting elastic anisotropy of foliated rocks based on laboratory measurements and macro-/microstructural observations (NW-Tauern Window, Austria)

Dustin Lang¹, Rebecca Kuehn¹, Rüdiger Kilian¹, and Michael Stipp¹

¹ *Martin-Luther University Halle-Wittenberg, dustin.lang@geo.uni-halle.de*

One of the main challenges in interpreting seismic data is dealing with elastic anisotropy, which is largely controlled by the modal content and CPO (crystallographic preferred orientation) of elastically anisotropic minerals as well as the rock microstructure. In order to determine the anisotropy of coaxially refolded schists from the NW-Tauern Window margin, we model seismic velocity data based on the micro- and macrostructure of the rocks and compare the results with lab experiments.

The CPO of millimeter-thick foliated rock cylinders was measured using synchrotron diffraction at DESY (Deutsches Elektronen-Synchrotron). CPOs were synthetically homogenized by weighted summation of rotated CPOs taking observed structures from thin sections and drill cores into account. The correlation of modeled CPOs with those, in which crenulated samples were measured directly, confirms the validity of this approach. From combined CPO data and modal compositions based on μ XRF, the seismic velocities are calculated. Layering effects are incorporated using computations according to Schoenberg and Muir (1989). For the laboratory experiments, the seismic velocity was measured on cubic rock samples with 42 mm side length in a true triaxial apparatus at Kiel University at confining pressures up to 600 MPa and temperatures up to 600°C.

Modeled velocities show $V_p(\max)$ values close to the experimentally measured intrinsic velocities. However, modeled $V_p(\min)$ values are higher than in the experiments. In the latter, $V_p(\min)$ is modified by reflection and dispersion due to the small wavelength in the apparatus set-up and compositional layering. Multiple folding at mm- to dm-scale reduces V_p -anisotropy mostly by increasing $V_p(\min)$. Layering increases the V_p -anisotropy by decreasing $V_p(\min)$. Increasing pressure and decreasing temperature decrease V_p -anisotropy and increase V_p . Hence, the presented modelling based on compositional and structural parameters is suggested to be a powerful method in order to predict elastic anisotropy of strongly anisotropic schists and phyllites.

References

Schoenberg, M. E., & Muir, F. (1989). A calculus for finely layered anisotropic media. *Geophysics*, 54(5), 581-589.

Limits of classical geothermal reservoir modelling in the Rhenohercynian Fold and Thrust Belt

Bernd Leiss¹ and David C.P. Peacock^{1,2}

¹ *Geowissenschaftliches Zentrum der Universität Göttingen, Strukturgeologie & Geothermik, Goldschmidtstraße 3, 37077 Göttingen, Deutschland*

² *Now at: School of Environmental and Life Sciences, University of Hull, Cottingham Road, Hull, HU6 7RX, UK*

Implementing use of deep geothermal systems in Europe beyond classical geothermal plays must include consideration of the geothermal potential of the Rhenohercynian Fold and Thrust Belt. This means considering a much larger variety of rock types, and characterising and conceptualising joint systems, faults, thrusts and folds at different scales to build up digital reservoir models for predicting the behaviour of open and closed loop systems, including responses to reservoir stimulation. We note two related mistakes commonly made in such studies: (1) failure to distinguish between different types of “fracture”, and (2) assuming that all “fractures” formed synchronously with, and are directly related to, the tectonic event that created the folds. These mistakes mean that the history of the structures and their influence on present-day fluid flow are misunderstood.

To start as simply as possible, we focused on the alternating greywacke and slate sequences that are typical of the Western Harz Mountains. We integrated 3D-field surveys from exposure to reservoir model scale, 3D-modelling, analogue studies and laboratory experiments to produce simple parametrised structures as input for reservoir models. Problems with inputting this information in discrete fracture networks included lack of specific information about the geometry and behaviour of open fractures in the sub-surface and the extensive computational time needed to model 3D characteristics of folds and fractures. As an alternative, we used Mohr circle modelling for open systems to test if economic parameters can be matched to argue for an exploration well. The geological and technical uncertainties have been, however, too high to demonstrate a reasonable business case for obtaining public and private funding up to now.

Brittle-ductile deformation of diopsidic clinopyroxene during incipient transformation of granulite to eclogite

Larissa Lenz¹, Sascha Zertani², Bernhard Grasemann³, Roland Stalder⁴, Luca Menegon⁵, and Anna Rogowitz¹

¹ *University of Innsbruck, Department of Geology; larissa.lenz@uibk.ac.at*

² *Stockholm University, Department of Geological Sciences*

³ *University of Vienna, Department of Geology*

⁴ *University of Innsbruck, Institute of Mineralogy and Petrography*

⁵ *University of Oslo, Department of Geosciences*

At dry lower-crustal conditions, clinopyroxene is considered to deform in a brittle manner as confirmed by experimental investigations. In contrast, field observations on Holsnøy, Norway, show bending of the presumably dry granulite foliation adjacent to eclogitic shear zones, indicating the macroscopically ductile deformation of coarse-grained clinopyroxene. In order to assess the deformation and reactions during incipient eclogitisation at the micro-scale, representative samples of weakly eclogitised granulite were examined using scanning electron microscopy, electron back-scattered diffraction mapping, electron microprobe analysis, and Fourier-transform infrared spectroscopy.

The results reveal the formation of garnet lamellae along {010} planes of diopsidic clinopyroxene. At a high angle to the {010} planes, en échelon microcracks formed during initial bending of the clinopyroxene, accommodating further bending. Along the en échelon microcracks, small garnet grains nucleate as well as amphibole and a second clinopyroxene, with higher Mg and lower Al contents. With increased strain, the microcracks link and evolve into micro-shear zones, which systematically widen with strain and eventually connect as networks. The microstructures of the host clinopyroxene suggest that the bending was accommodated by combined flexural flow along lamellar garnet of the {010} planes and crystal-plastic processes. In contrast, the new grains nucleating at the micro-shear zones indicate diffusion-related processes.

The observed microstructures indicate the presence of water, either as external fluids, infiltrating through the en échelon microcracks, or as minor amounts of OH-groups stored in the nominally anhydrous clinopyroxene. First Fourier-transform infrared spectroscopy results suggest that the nucleation of amphibole might be facilitated by the incorporated OH in the diopsidic clinopyroxene.

Our results demonstrate the interplay of brittle and ductile deformation at microscale during incipient eclogitisation. Moreover, the presence of incorporated OH-groups in clinopyroxene facilitates the observed reactions and deformation, suggesting that the amount of external fluids required during eclogitisation may be less than previously assumed.

Margins, Oceans, and Compression: What Controls Collision Architectures?

Iskander A. Muldashev¹ and Thorsten J. Nagel¹

¹ *Institut für Geologie, TU Bergakademie Freiberg, iskander.muldashev@geo.tu-freiberg.de*

The transition from subduction to collision marks a pivotal geological transformation. The collision process is associated with series of events, which include exhumation of continental high-pressure (HP) and ultra-high-pressure (UHP) units, nappe stacking, increased magmatic activity, rapid rise of topography among others.

We use numerical modeling to address the dynamics of continental margin subduction and the subsequent transition to collision with particular attention to the deep subduction and exhumation of continental crust. The models are designed to investigate how a lubricating sedimentary layer at the plate interface, the width of the subducting passive margin, the crustal thickness of the subducting plate, and the overall tectonic compression of the collision control the history and resulting architecture of continental HP units.

We use the thermo-mechanical marker-in-cell Finite Element Method (FEM) code SLIM3D (Popov and Sobolev, 2008). The method employs a visco-elasto-plastic rheology and accounts for fundamental metamorphic phase transitions. The model domain is 2000 km wide and 1000 km deep. The models employ force boundary conditions instead of conventional velocity boundary conditions to simulate mid-ocean ridge push force and subduction pull force caused by neighboring slabs.

Modelling results suggest that exhumation of continental HP and UHP units from great depth to near the surface happens only during rapid, large-scale movements in the collision zone. Such events place exhumed units consistently on top of the accreted crust. The deep subduction of large amounts of continental crust is further facilitated by wide margins of thinned upper crust, as thinned upper crust is rheologically attached to the downgoing slab while regular crust contains a weak detachment horizon in the middle crust, which promotes shallow accretion.

Interplay of metamorphism and deformation mechanisms in eclogite - Implications on transient mechanical behaviour at convergent settings.

Anna Rogowitz¹, Simon Schorn², and Benjamin Huet³

¹ *Department of Geology, University of Innsbruck, Innsbruck, Austria,*
anna.rogowitz@uibk.ac.at

² *Institute of Geosciences, University of Mainz, Mainz, Germany,*

³ *Geosphere Austria, Vienna, Austria*

In convergent settings, such as subduction and collision zones, dry mafic rocks are subducted to high pressures and subsequently transformed into eclogite. While eclogite protoliths (i.e., basalt, gabbro, granulite) are assumed to be rather strong, their high-pressure equivalent (i.e., eclogite) frequently hosts ductile shear zones. Numerous studies have investigated eclogite deformation behavior to identify the processes responsible for strain localization at high pressure, yet results remain ambiguous. This apparent contradiction raises fundamental questions about the factors controlling the deformation of eclogite.

Here, I present two case studies from the eclogite type locality of the Saualpe–Koralpe Complex (Eastern Alps, Austria). Integrated field, microstructural, and geochemical investigations document strong interactions between metamorphic reactions and deformation processes operating under eclogite-facies conditions.

In the first case study, fluid-assisted syntectonic prograde eclogitization was initially accommodated by diffusion creep and dissolution–precipitation creep, leading to a pronounced shape-preferred orientation of the dominant minerals. Continued prograde metamorphism resulted in progressive dehydration and partial melting of the eclogite. A concomitant increase in pore-fluid pressure induced brittle failure and enabled the precipitation of eclogite-facies mineral assemblages in synmetamorphic veins.

The second case study focuses on an eclogite-facies shear zone containing two eclogite-facies lithologies: an eclogite matrix with interlayered zoisite–hornblende–garnet enclaves. Stress concentrations along eclogite–enclave contacts promoted recrystallization of the weaker eclogite assemblage. The resulting fabric became dominated by a nearly euhedral clinopyroxene matrix that deformed primarily by grain-size-sensitive grain boundary sliding. Prograde melting also occurred in this case; however, here the melt formed an interconnected network that further weakened the eclogite.

These results highlight the critical role of compositional heterogeneities and metamorphic reactions in controlling strain localization under high-pressure conditions. The identified sequence of deformation mechanisms leads to transient mechanical behaviours that may significantly influence the dynamics in convergent tectonic settings.

Variscan tectonics of the Elbe Zone – Pervasive strike-slip overprint of a pre-existing accretionary complex

Lea Schulze and Uwe Kroner

Department of Geology, TU Bergakademie Freiberg, B.-v.-Cotta-Strasse 2, D-09599 Freiberg, Germany

The architecture of Saxo-Thuringia (Central European Variscides) is generally characterized by SW-NE striking tectonic units. An exception to this is the NW-SE oriented Elbe Zone which evolved during the final stage of the Variscan orogeny as a dextral strike-slip zone juxtaposing the Erzgebirge and the Lausitz block with the Elbtalschiefergebirge (ETS) in between. Based on a revised geological model of the ETS [1], here we discuss the evolution of this region in a broader context.

Dextral shearing of the Elbe Zone (340-330 Ma) is co-genetic to the final HT-LP metamorphic overprint of upper crustal allochthonous units and contemporaneous to the rapid northwest directed exhumation of the “hot” Saxon Granulite Massif, the synkinematic intrusions of the Meissen Massif and the granite of Berbersdorf. This tectonothermal overprint affected the already metamorphosed ETS together with discordantly overlying synorogenic sediments. Strike-slip related juxtaposition of the ETS with the medium- to high-grade metamorphic Erzgebirge complex occurred in the upper crust utilizing the ductile to brittle Mid-Saxon Shear Zone. Ductile shear in the Elbe Zone terminated prior to the post-kinematic emplacement of the Sayda-Berggießhübel dyke swarm (314 and 311 Ma [2]).

Thus, the formation of the Elbe Zone postdates peak metamorphism of HP-UHT Saxon granulites and the UHP metamorphism in the Erzgebirge at ca. 340 Ma as well as the low-grade metamorphism of the Palaeozoic sequences of the ETS. The lithologies of the ETS resemble the schist belts of Saxo-Thuringia further to the southwest. These regions are characterized by heterogenous accretionary tectonics associated with Late Devonian bimodal magmatism and marine facies differentiation. This in turn was followed by Early Carboniferous southwest-directed nappe stacking contemporaneous with NE-SW oriented dextral strike-slip tectonics [3].

Because the architecture of the ETS is dominated by the NW-SE directed ductile shear of the Elbe Zone, its original geometry as a SW-vergent accretionary belt is almost completely obscured. Both stages, however, are necessary to explain the complex history of this part of the Elbe Zone.

References

- [1] Schulze, L. M., & Kroner, U. (2026). The Variscan architecture of the Elbtalschiefergebirge and its periphery, Saxo-Thuringian Zone. *Zeitschrift der Deutschen Gesellschaft für Geowissenschaften*. doi:10.1127/zdgg/0512
- [2] Tichomirowa, M., Käßner, A., Repstock, A., Weber, S., Gerdes, A., & Whitehouse, M. (2022). New CA-ID-TIMS U–Pb zircon ages for the Altenberg–Teplice Volcanic Complex (ATVC) document discrete and coeval pulses of Variscan magmatic activity in the Eastern Erzgebirge (Eastern Variscan Belt). *International Journal of Earth Sciences*, 111(6), 1885-1908. doi:10.1007/s00531-022-02204-2
- [3] Hahn, T., Kroner, U., & Melzer, P. (2010). Early Carboniferous synorogenic sedimentation in the Saxo-Thuringian Basin and the adjacent Allochthonous Domain. In *Pre-Mesozoic Geology of Saxo-Thuringia: From the Cadomian Active Margin to the Variscan Orogen*. (pp. 171-192): Schweizerbart, Stuttgart.

Small Inclusions, Big Implications: Tracing the Polymetamorphic Variscan Evolution of the Southern Bohemian Massif

Dominik Sorger^{1,2}, Christoph A. Hauzenberger¹, Fritz Finger³, Manfred Linner⁴, Christoph Iglseider⁴, Etienne Skrzypek¹, Simon Schorn⁵, and David Günzler^{1,2}

¹ *University of Graz, dominik.sorger@uni-graz.at*

² *University of Göttingen*

³ *University of Salzburg*

⁴ *GeoSphere Austria*

⁵ *JGU Mainz*

The Moldanubian sector of the Variscan Orogen represents a complex mosaic of peri-Gondwanan terranes, amalgamated during a prolonged tectonometamorphic cycle. These high-grade rocks record a polyphase history spanning over 60 Ma, yet unraveling the precise succession of burial, collision and exhumation is complicated by pervasive high-temperature overprinting. Here, we present an integrated study using chemically and texturally zoned garnet porphyroblasts and associated inclusions, coupled with texturally related monazite petrochronology and the analysis of crystallized melt inclusions (nanogranitoids) from the Bohemian Massif.

Our data document a discontinuous tectonometamorphic evolution characterized by three discrete stages. Earliest garnet growth records high-grade metamorphism at ~370 Ma, marking the initial subduction of peri-Gondwanan crust. This is succeeded by the dominant Visean collision (~340 Ma), where crustal thickening led to medium-pressure/high-temperature conditions and partial melting. Subsequent rapid exhumation triggered near-isothermal decompression, recorded in rare aluminous lithologies by cordierite-spinel symplectites. The orogenic cycle terminates with a distinct late-stage low-pressure/high-temperature overprint at ~312 Ma. This indicates a significant advective heat influx, likely related to mantle delamination, during the final waning stages of convergence.

To resolve the precise onset and chemistry of melting, we target nanogranitoid inclusions (quartz, feldspar polymorphs, mica, \pm carbonates) preserved within chemically distinct domains of both monazite and garnet. By correlating monazite domains dated at ~370 Ma with the first garnet generation, and ~340 Ma domains with the second, we can track the redistribution of REE, Th and U during specific mineral breakdown reactions. Systematically analyzing these inclusions in their textural context not only enhances our understanding of monazite stability in melt-bearing systems but establishes this accessory mineral as an indispensable archive for deciphering the temporal dynamics of crustal differentiation.

Intraplate paleoseismicity in low seismic settings of Central Europe (Germany)

Vanessa Steinritz¹ and Klaus Reicherter¹

¹ RWTH Aachen University, Inst. of Neotectonics and Natural Hazards

k.reicherter@nug.rwth-aachen.de

Intraplate regions present significant challenges for seismic hazard analyses due to their low seismicity and limited data on active faults. In such regions, strong earthquakes with surface ruptures are rare, with recurrence intervals often spanning several thousand years. Maximum earthquake magnitudes are typically derived from seismic records covering approximately the last 100 years and are frequently incorporated into hazard calculations. To address these challenges, we employ morphotectonic studies, shallow geophysics and paleoseismic trenching, and DInSAR modeling in the Lower Rhine Graben (LRG) in Germany. We present new paleoseismic data and critically assess recurrence intervals in intraplate settings in the context of seismic hazard assessment. The LRG is a seismically active intraplate region that has experienced damaging historical earthquakes, such as the Düren event in 1756 and the Verviers event in 1692, both with magnitudes ~Mw 6.5; and lastly the Roermond 1992 event without surface rupture. The LRG is bordered to the west by the Feldbiss Fault Zone, which has been extensively studied, particularly in its southern section, revealing late Holocene surface-rupturing faults, but also evidence of older events further underscores the long-term seismic activity. We also trenched the adjacent Sandgewand Fault and the Rurrand Fault, uncovering additional paleoseismic evidence for surface-rupturing earthquakes. We were able to construct a robust time-frame for the earthquake history including archaeological data. In the last 50 years, considerable aseismic creep has been accumulating localized slip of partly more than 90 cm at faults due to groundwater extraction and sediment compaction in adjacent lignite mines. Our results indicate that several major faults ruptured during large earthquakes, but remain currently reactivated by anthropogenically induced subsidence. This dual control/overlap of coseismic and induced reactivation emphasizes the urgent need to monitor and to integrate both processes into seismic hazard assessments for the Lower Rhine Graben.

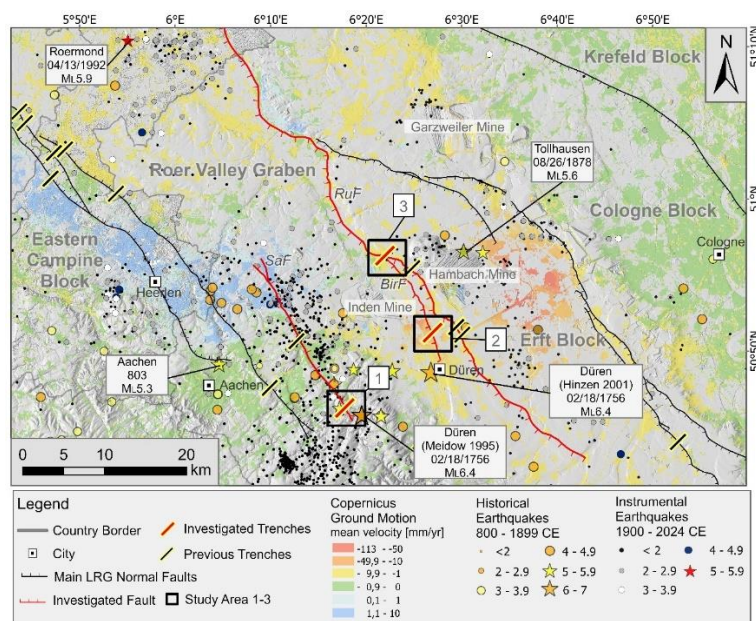


Figure 1: Overview of the study region across the Sandgewand Fault (1), Birkesdorfer Fault (2), and Rurrand Fault (3), current seismicity, historical recorded events and mining-induced ground motion data from Copernicus InSAR data covering the period 2019–2023 are shown (subsidence: red, uplift: blue).

Birth, Life and Fate of a Hadal Basin in the Japan Trench – First Results from IODP³-Expedition 503

Stipp, M. ^{1,2}, Fukuchi, R. ^{1,3}, Strasser, M. ¹, Ikehara, K. ¹, Maeda, L. ¹, Bartos, M. ¹, Bowden, S. ¹, Chang, Y.-C. ¹, Chu, N.-C. ¹, Cornard, P. ¹, Diz, P. ¹, Eguchi, N. ¹, Fujishima, S. ¹, Garrido, S. ¹, Gea, M. ¹, Hanifah, D. ¹, Hashimoto, Y. ¹, Hoshino, T. ¹, Hovikosko, J. ¹, Huang, T.-H. ¹, Iizuka, M. ¹, Ishizawa, T. ¹, Kitazato, H. ¹, März, C. ¹, Muthre, M. ¹, Okutsu, N. ¹, Pizer, C. ¹, Robustelli Test, C. ¹, Satoguchi, Y. ¹, Shorrock, A. ¹, Steward, M. ¹, Strachan, L. ¹, Toczko, S. ¹, Xiao, W. ¹, Yamagishi, S. ¹, Yamamoto, Y. ¹, Yokoyama, Y. ¹, Zabel, M. ¹, Zhao, Y. ¹

¹ IODP³-Expedition 503 Science Team

² Martin Luther University Halle-Wittenberg, Germany, Michael.Stipp@geo.uni-halle.de

³ Naruto University of Education, Japan

IODP³-Expedition 503 focused on drilling in the hadal basin of the Central Japan Trench near the hypocenter of the Tohoku-Oki megathrust earthquake of March 11, 2011. Short historical records limit our knowledge about magnitude and recurrence of such catastrophic events. The goal of IODP³-Exp. 503 was to significantly extend this record for the Japan Trench towards greater depth.

At Site C0028, five boreholes were drilled at a water depth of ~7609 m. Drill core C0028B, reaching a maximum depth of 178 m below seafloor (mbsf), covers the entire trench fill succession. It displays an angular unconformity, beneath which significantly older sediments of the incoming plate occur. Paleomagnetic data of the latter imply that they were deposited prior to the Matuyama–Brunhes polarity reversal at ~773 ka. The sedimentary succession is well-preserved and characterized by volcanoclastic-rich layers overlain by mixed siliciclastic and biogenic deposits. The numerous turbidites contained therein, which are potentially earthquake related, are defined by thin coarse-grained basal layers capped by thick, homogeneous fine-grained deposits.

Bedding plane orientation is largely horizontal, but at greater depth, particularly below the unconformity (~169 mbsf), there is a significant deviation towards slightly to moderately dipping strata. In this lower part of the succession, the sediments are weakly deformed by sediment-filled veins and some minor faults. These form two distinct sets of conjugate normal faults, presumably representing bend faulting of the incoming Pacific Plate. The hadal trench basin most likely originated from a graben structure developed during plate bending between the outer rise and the plate boundary. Correspondingly, the sedimentary succession reflects the initiation and subsequent infill of this basin.

The sedimentary succession with micropaleontological, volcanoclastic and paleomagnetic data, as well as the structural results, could contribute to significantly expanding the records of tsunamigenic slip in the Japan Trench and improving the general understanding of earthquake recurrence intervals and hazards at active continental margins.

Intrusive and extrusive evolution of two Late Carboniferous calderas in the NW Bohemian Massif

Filip Tomek^{1,2}, Petr Vitouš^{1,2}, and Irena Olšanská¹

¹ *The Czech Academy of Sciences, Institute of Geology, Prague, Czech Republic, filip.tomek@natur.cuni.cz*

² *Institute of Geology and Paleontology, Faculty of Science, Charles University, Prague, Czech Republic*

The Carboniferous Altenberg–Teplice (ATC) and Tharandter Wald (TWC) calderas formed during post-collisional Variscan magmatism in the NW Bohemian Massif. We synthesize advances from the last 4–6 years and outline future research directions. Pre-caldera units emplaced between ca. 325–319 Ma comprise composite monzogranite plutons and a volcano-sedimentary complex (ATC). They differ geochemically from younger caldera-related ignimbrites, dikes, and shallow-level plutons. Volcanism associated with ATC likely began with small-volume ignimbrites prior to 314 Ma, whereas major caldera-forming eruptions in both systems culminated at ca. 314 Ma. Magnetic fabric and paleomagnetic studies constrain pyroclastic current directions, rheomorphic bending, and extensive hydrothermal overprint, also indicating that most ATC ignimbrites were sourced from a rhyolite dike swarm. The areal extent, thickness, and grain-size isopachs show that ATC outflow ignimbrites traveled predominantly to the SE, feeding co-ignimbrite ash fall into Bohemian Carboniferous basins. The cumulative dense-rock equivalent volume of ATC products exceeds 350 km³. The final caldera collapse triggered emplacement of cumulate-like mushy magma along ring faults. Subsequent shallow-level Li-mica and biotite granites with extensive Sn–W–Li mineralization record the post-collapse evolution. Structural analysis of syn-caldera faults, intrusive geometries, and dike-swarm fabrics demonstrates that caldera emplacement was largely controlled by a Riedel Fracture System compatible with dextral motion on the ~NW–SE Elbe Shear Zone. The stress regime was characterized by a ~ N-S-trending maximum horizontal stress (σ_1) and ~E–W minimum horizontal stress (σ_3), consistent with the regional field. Both calderas were sourced from medium- to high-temperature (~770–930 °C) felsic lower-crustal magmas, as indicated by Ti-in-zircon, zircon saturation thermometry, and thermoremanent magnetization data. The time-averaged behavior of the geomagnetic field during caldera activity is addressed in a companion presentation.

A virtual KTB (Kontinentale TiefBohrung): The ultimate benchmark for apatite fission track annealing?

Florian Trilsch¹, Raymond Jonckheere¹, and Thorsten Nagel¹

¹ *Institut für Endogene Geologie, TU Bergakademie Freiberg* florian.trilsch@geo.tu-freiberg.de

Apatite fission track modeling reconstructs the low-temperature histories of geological samples based on measurements of the lengths of etched confined fission tracks. Modeling results are only as good as the underlying equations that describe track annealing. Annealing equations fitted to data acquired in high-temperature laboratory annealing experiments over short time-scales need to be verified on geological benchmarks, i.e., on data from settings where the thermal histories are known from independent geological and thermochronological information. A few separate non-ideal high and low-temperature benchmarks have been proposed. For the KTB Borehole, independent geological data are consistent with thermal steady-state since the Late Cretaceous-Paleocene. Thus, the KTB borehole, with nearly mono-compositional Fluorine-apatites, is a promising candidate benchmark over the entire range of fission track annealing. For optimizing our length measurements, we use deep ion irradiation and record and measure sub-horizontal confined tracks after an etch time of 40 seconds on apatites from the surface down to 4000 meters depth. This allows us to increase the number of measured lengths compared to earlier studies significantly. At the same time, effective etch time calculations enable us a quantitative criterion for track selection. We create a Virtual KTB comprising images of each measured confined track together with our measurements and place it on a public server. This allows other scientists to remeasure the KTB length profile using their own selection criteria and measurement techniques. This could lead to a consensus on the KTB as a reference dataset for geological annealing.

Late Carboniferous geomagnetic field events captured by Altenberg–Teplice Caldera, Bohemian Massif

Petr Vitouš^{1,2*}, Michael S. Petronis³, Marine S. Foucher³, and Filip Tomek^{1,2}

¹ *The Czech Academy of Sciences, Institute of Geology, Prague, Czech Republic,*
vitous@gli.cas.cz

² *Institute of Geology and Paleontology, Faculty of Science, Charles University, Prague, Czech Republic*

³ *Environmental Geology, Natural Resources Management Department, New Mexico Highlands University, Las Vegas, NM 87701, USA*

The Altenberg–Teplice Caldera is an erosional relic of a volcano-plutonic edifice in the NW Bohemian Massif that was active during the terminal phases of Variscan orogeny. The paleomagnetic data record a previously unrecognized Late Carboniferous geomagnetic field behavior during the Kiaman Reverse Superchron. Through thermal and alternating-field demagnetization, along with magneto-mineralogical analyses, various parts of the caldera were investigated, including the syn-caldera rhyolite dike swarm, intra- and extra-caldera rhyolite ignimbrite, and the post-caldera microgranite ring dikes. Most of the examined samples yield a primary thermoremanent magnetization carried by a mixture of single- to multi-domain low-Ti titanomagnetites. The obtained paleomagnetic directions range from those consistent with the expected primary Late Carboniferous geomagnetic field to intermediate directions with $>45^\circ$ deviation from dipole states. We interpret these intermediate directions, captured by certain parts of the intra-caldera ignimbrites and younger syn- to post-collapse ring dikes, as intermediate field behavior intervals during the Late Carboniferous within the Kiaman Reversed Polarity Superchron.

Our new data, supported by published cross-cutting relationships and high-precision geochronology, indicate that the two events occurred between approximately 314.7 and 313.04 Ma and between 314.7 and 312.6 Ma, considering the 2σ analytical uncertainty (Tichomirowa et al., 2025; Opluštil et al., 2016). The former interval corresponds to the main eruptive phase, while the latter reflects the emplacement of the ring dike system. Both intervals of intermediate directions fall within chron PE5r and marginally within chron PE6.1n, interpreted as excursions of the magnetic field from its typical dipole state. The Altenberg–Teplice Caldera thus provides new paleomagnetic evidence that challenges the long-standing assumption of generally reversed polarity over the ~55-million-year duration of the Kiaman Superchron and offers new insights into the variability of geomagnetic behavior during this interval in Earth's history.

References

- Tichomirowa et al. (2025). *Int. J. Earth Sci.*, 114, 531–551.
Opluštil et al. (2016). *Earth-Sci. Rev.*, 154, 301–335.

A juvenile arc terrane in the Mid-German Crystalline Zone – constraints from zircon U-Pb-Hf isotope data and implications for pre- to syn-Variscan evolution

Armin Zeh¹, Marius Beck², Matthias Hinderer², Henri P. Meinass², and Axel Gerdes³

¹ KIT Karlsruhe, armin.zeh@kit.edu

² TU Darmstadt, us.beck@t-online.de, hinderer@geo.tu-darmstadt.de, meinass@geo.tu-darmstadt.de,

³ Frankfurt University, gerdes@em.uni-frankfurt.de

Presently, little is known about the zircon age-Hf isotope record of (meta)sedimentary rocks exposed in the southernmost part of the Mid-German Crystalline Zone (MGCZ) and adjacent Rhenohercynian Domain, preventing detailed reconstructions of the geodynamic evolution in Central Europe. In this study, such data are presented from Late Devonian to Viséan metagreywackes, metapelites and granite gneisses of the Palatinate Forest (MGCZ) and the Harz Mountains (Rhenohercynian). These provide evidence that sediments in both realms were sourced from a so far unrecognized, juvenile oceanic arc terrane, which initially was formed at 490-570 Ma (ϵ_{Hf} up to +13.0), and internally reworked at ca. 500, 400, 370 and 335 Ma (ϵ_{Hf} = +2.0 to +8.4), prior to Variscan collision and post-kinematic magmatism at 330 Ma. Late Devonian arc reworking is reflected by the ca. 370 Ma Albersweiler granite gneiss showing superchondritic ϵ_{Hf} of +3.6 to +7.7, and older reworking by the detrital zircon record. Results of data compilation further suggest that the oceanic arc terrane remained widely isolated from continental input within the Prototethys/Rheic ocean realm until its collision with Avalonia at 335 Ma, but also that relics of the arc system became widely dispersed within the Saxothuringian, Rhenohercynian and Moldanubian domains during Variscan collision and collapse.

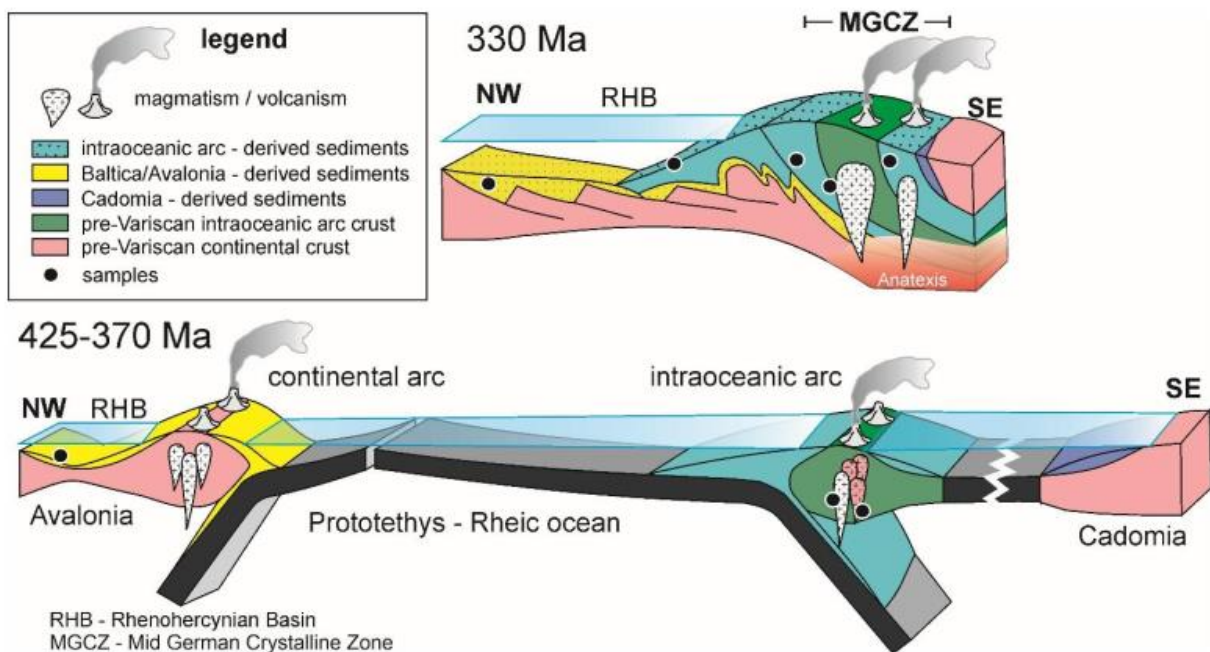


Figure 1: Geodynamic evolution of the southern part of the Mid-German Crystalline Zone during the Devonian to Viséan.

Posters

Experimental and microstructural study on the effect of second phase particles on compaction mechanisms of halite

Marleen Bodenstein¹, Rüdiger Kilian¹, André Eschenröder¹, Florian Fritz¹, Maximilian Köhne², and Michael Stipp¹

¹ Martin-Luther-University Halle-Wittenberg, marleen.bodenstein@student.uni-halle.de

² Helmholtz Centre for Environmental Research GmbH - UFZ

Dissolution-precipitation creep is an important deformation mechanism in many geomaterials and across a wide range of crustal conditions; from initial compaction in sediments up to deformation of polymineralic rocks at high grade conditions. The presence of second phase particles and phase boundaries is envisaged to significantly modify creep rates. Unfortunately, the effect is difficult to explore experimentally in most silicate systems at laboratory time scales. However, halite with mica grains as second phase particles serves as suitable analogue.

In this study, cylindrical samples (diameter of 70 mm, height of 125 mm) containing mixtures of ground halite with a grain size of 2-4 mm (pre-dried, 1 wt.-% water-added) and various volume fractions of mica (5, 15 vol.-%) were compacted in a 5000 kN-piston-cylinder apparatus. The large sample size was chosen such that the grain size can be large enough to allow for multiple deformation modes, but experiments are not affected by boundary conditions. Experiments were conducted at room temperature and at constant force (6, 40, 60 kN) as well as constant normal stress conditions (2, 6, 15 MPa). For comparable loads (40 kN ~ 15 MPa), similar displacement rates for both experimental conditions were achieved, though theoretically with constant force boundary conditions microstructural steady-state cannot be attained. For high stress experiments at 60 kN (~ 20 MPa), the stress exponent has a value of around 20, indicating rate-independency. With decreasing stress to 2 MPa, the exponent evolves to 1.7. Thus, dissolution-precipitation becomes an increasingly dominant deformation process, although fracturing is still active.

All samples were analyzed post-mortem using computed tomography (1 voxel=40 µm). Tomography data shows fractures perpendicular to the surface of halite grains. Additionally, halite-mica boundaries, which are not parallel to (100) of halite as well as indented grains and rounded edges are observed, indicative of dissolution-precipitation. The strain rate is affected by the addition of mica ($1 \cdot 10^{-9} \text{ s}^{-1}$ with 5 vol.-% mica, $3 \cdot 10^{-9} \text{ s}^{-1}$ with 15 vol.-% mica) suggesting a combined mechanism of fracturing and dissolution-precipitation. Hence, second phase particles may not only control the strain rate and strength of rock salt, but also the activity of certain deformation processes in creep tests.

Tectono-Structural Evolution of the Pre-Devonian Basement, Inner Billefjorden, Svalbard

Muriel Bühlhoff^{1,3}, Aleksandra Smyrak-Sikora², Kim Senger³, and Hannah Pomella¹

¹ *University of Innsbruck, Austria, muriel.buelhoff@student.uibk.ac.at, hannah.pomella@uibk.ac.at*

² *Norwegian University of Science and Technology, Trondheim, Norway, aleksandra.a.smyrak-sikora@ntnu.no*

³ *University Centre in Svalbard, Longyearbyen, Norway, kims@unis.no*

Several long-lived N–S-striking lineaments crosscut Spitsbergen, with the Billefjorden Fault Zone (BFZ) being the most studied one. The BFZ records multiple tectono-thermal events, originating in the Caledonian shear zone. Following evolution reflects reverse faulting during the Late Devonian Svalbardian event, normal faulting during the Late Carboniferous rifting, hydrothermal fluid flow synchronous with the emplacement of the Early Cretaceous High Arctic Large Igneous Province, and the faults reactivation during the Paleogene Eureka shortening. The Paleo- to Mesoproterozoic pre-Devonian basement consist of quartzite with amphibolite bands, marbles, garnet–mica schist, gneisses, and sandstones metamorphosed in greenschist to amphibolite-conditions. It preserves evidence of all younger tectono-thermal events, through which it was ultimately exhumed. Despite its significance, the metamorphic basement in Billefjorden remains understudied.

In this study we investigate the structural architecture and timing of the transition from ductile to brittle deformation recorded in the metamorphic basement. We apply a multiscale approach that integrates aerial and drone-based imagery with detailed field observations, structural and lithological mapping, microstructural analyses, and apatite and zircon fission-track dating. Five digital outcrop models were generated from the acquired imagery, and 19 thin sections were prepared. Based on our mapping, we provide an updated geological map of the metamorphic units. Structural mapping reveals the presence of stretching lineations and multiple generations of (folded) foliations. Mixed ductile–brittle structures constrain the transition, whereas fractures, variably oriented brittle fault planes, slickensides, and slickenlines document subsequent brittle deformation. The timing of basement exhumation will be further constrained by zircon and apatite fission-track analyses of 15 selected samples.

In this contribution, we present preliminary structural and petrological results that provide new insights into the exhumation history of the metamorphic basement exposed along the BFZ. The thermochronological data presently under analysis will complement this data allowing to constrain the tectonic evolution of the region.

Development of a polyphase basement: Ograzhden Unit, SW Bulgaria

Alex Jensen¹, Jan Pleuger¹, Xin Zhong¹, Elis Hoffmann¹, Stoyan Georgiev², and Jessica Stammeier³

¹ Freie Universität Berlin, alejjen@proton.me

² Geological Institute „Stashimir Dimitrov”, Bulgarian Academy of Sciences

³ GFZ Helmholtz Centre for Geosciences

Polyphase orogens are products of recurring deformation, metamorphism, remelting and crustal recycling. The Ograzhden Unit in SW Bulgaria represents an amalgamation of Gondwana-derived crustal material and Triassic granites (Peytcheva et al., 2015), and was molded through pre-Variscan, Variscan and Alpine orogenies. The bulk of the basement consists of predominantly Upper Ordovician granites, with some Cambrian granitoids and Precambrian migmatites, slivers of amphibolites and paragneisses, intruded by Triassic plutons and later affected by Oligocene volcanism. Known metamorphic stages comprise a high-grade pre-Variscan anatexis, Variscan (U)HP event recorded in the Gega eclogite (Trapp et al., 2019) and loosely constrained low-grade Alpine deformation (Kilias et al., 1999; Kounov & Gerdjikov, 2024).

Using structural, petrological, geochronological and geochemical methods, we trace the multiphase magmatic-metamorphic evolution, and constrain the style and timing of deformation. We present new data on the U-Pb ages of the basement: the Nikudin granite dated 444.8 ± 1.5 Ma – which suggests it records both Variscan and Alpine deformation. Detrital ages of the Lebnitsa metasediment show maximal depositional ages of 424 Ma and Gondwana-affinity. Zircon metamorphic overgrowth (clustering at 330 Ma) in pegmatite samples confirms the persistence of the Variscan metamorphism throughout the bulk of the basement, however the high pressure metamorphic grade known from Gega has not yet been observed. Mineral assemblage thermodynamic modelling and quartz-in-garnet Raman elastic barometry suggest a metamorphic event at ≥ 1.2 GPa and 600°C recorded in amphibolites and paragneisses, which we interpret as Variscan. Alpine deformation and metamorphism under lower amphibolite-upper greenschist facies conditions is reflected in the Triassic Igralishte granite. Similar conditions are also recorded by secondary mineral assemblages in the Lebnitsa metasediment. The evolution of the Ograzhden Unit thus represents a polyphase metamorphic and magmatic development of orogenic continental crust, recording the deformation of at least three major orogenies and five magmatic stages.

References

- Kilias, A. & Falalakis, G. & Mountrakis, D. (1999). *IJES*. 88, 513-531.
 Kounov, A. & Gerdjikov, Ia. (2024). *Geologica Balcanica*. 53, 29-85.
 Peytcheva, I. & Macheva, L. & von Quadt, A. & Zidarov, N. (2016). *Geologica Balcanica*. 44, 1-3.
 Trapp, S. & Janák, M. & Faßmer, K. & Froitzheim, N. & Münker, C. & Georgiev, N. (2020). *Terra Nova*, 33, 174–183

Previously unrecognized high-pressure metamorphism in the Eastern Erzgebirge.

Martin Keseberg¹, Tristan Lange¹, Tim Koark¹, Till Burock¹, and Thorsten Nagel¹

¹ *TU Bergakademie Freiberg, Martin.Keseberg@geo.tu-freiberg.de*

The vast majority of tectono-metamorphic studies in the Erzgebirge have either focused on its central or western parts. Meanwhile, almost no modern studies have dealt with the metamorphic evolution of the eastern part. This lack of data has significant effects on existing tectono-metamorphic models of the Erzgebirge. For instance, eclogites were only described after the development of most of these models, leading to false interpretations of the extent of high-pressure units in the Erzgebirge as a whole. Most of the eclogites in the Eastern Erzgebirge occur in similar tectonic levels as those of the Western Erzgebirge, which, in addition to our pressure-temperature data, indicates a relatively coherent high-pressure unit. We also present first descriptions of omphacite-garnet bearing assemblages from the structurally deeper, internal levels of the Lauenstein-Dome. The Lauenstein-Dome is seen as part of the lower-most exposed unit of the Erzgebirge, which is commonly regarded as being affected only by amphibolite-facies metamorphism with no high-pressure history and has even been interpreted as Cadomian basement.

In-Sequence Thrusting and Triangle Zone Development in the External Dinarides: Constraints from 2D Kinematic Forward Modelling of a cross section around the Drežnica Canyon, Bosnia and Herzegovina

Marah Kieckbusch, Philipp Balling, and Kamil Ustaszewski

Institut für Geowissenschaften, Friedrich-Schiller-Universität Jena, Burgweg 11, 07749 Jena, Germany

The Dinarides fold-and-thrust belt formed as a result of the Late Cretaceous collision between the Adriatic microplate and Eurasia and was further shaped by Paleogene post-collisional shortening. During the Middle Eocene, deformation propagated southwestward, progressively incorporating the external domains of the Mesozoic Adriatic carbonate platform into the fold-and-thrust belt by predominantly SW-vergent, in-sequence thrusting. However, official geological maps of the Drežnica Canyon area (central External Dinarides, Bosnia and Herzegovina) reveal a shift in transport directions within the canyon, indicating complex deformation geometries that contrast with the regional structural style and have not yet been systematically studied.

To evaluate the structural architecture and kinematic evolution of this area, we constructed an ~80 km long geological profile, extending from the Drežnica Canyon to the Pelješac Peninsula (Croatia). Official geological maps at the scale of 1:100.000 served as primary data sources and were complemented by additional fieldwork to document shear-sense indicators and verify mapped structures. Subsequently, 2D kinematic forward modelling was employed to test alternative deformation scenarios and to constrain the geometry and position of major detachment horizons along the newly constructed cross section.

The resulting model confirms the contrasting structural styles between its northern and southern segments. In its central and southern parts, Paleogene shortening was accommodated by a relatively uniform system of SW-vergent thrusts that propagated in sequence and detached within Lower Triassic marly limestone sequences. In contrast, the northern segment (Drežnica Canyon) is characterized by a triangle structure involving a top-to-the-NE-vergent backthrust that cuts across the northerly adjacent SW-vergent thrust system. This structure represents localized out-of-sequence thrusting superimposed on an overall in-sequence thrust belt. Total Eocene–Oligocene shortening across the entire cross-section is estimated at ~ 25 km.

G.O.Joe: A new online tool for LA-ICP-MS data reduction

Joachim Krause¹, Florian Altenberger², Thomas Auer³, Alexander Auer³, and Jasper Berndt⁴

¹ *Helmholtz-Zentrum Dresden-Rossendorf, Helmholtz Institute Freiberg for Resource Technology, Chemnitzer Str. 40, 09599 Freiberg, Germany, joachim.krause@hzdr.de*

² *Montanuniversität Leoben, Department Applied Geosciences and Geophysics, Chair of Resource Mineralogy, Peter Tunner-Straße 5, 8700 Leoben, Austria*

³ *Moonshot Pioneers GmbH, Dorfbeuern 35, 5152 Dorfbeuern/Salzburg, Austria*

⁴ *University of Münster, Institute for Mineralogy, Corrensstraße 24, 48149 Münster, Germany*

The coupling of laser ablation systems with inductively coupled plasma-mass spectrometers (LA-ICP-MS) was introduced in the 1980s. Since then, this technique has become indispensable for rapid in-situ trace element and isotopic analysis of both natural and synthetic solid samples. Its applications extend across various fields, including chemistry, materials science, geosciences, biological and environmental analysis, bio-imaging and forensic investigations. However, analytical advances are still needed to address challenges in trace element analysis using LA-ICP-MS, such as those caused by interferences.

The novel, non-commercial software tool G.O.Joe (Altenberger et al. 2024) is designed to facilitate the calculation of trace element mass fractions in solid samples obtained by LA-ICP-MS analysis. It is written in the Dart programming language using the Flutter framework and operates entirely as a web-based application (i.e., no installation required). Since the data processing is performed on the user's computer, there is no need to upload data to the G.O.Joe-server, maximizing data security. In addition to enabling the quick and efficient processing of large datasets, G.O.Joe includes various optional interference corrections methods.

G.O.Joe's intuitive user interface simplifies the workflow during data evaluation, allowing for straightforward selections of peak- and background signals, importation of instrument settings, reference material compositions, and mass fractions of the internal standard to convert the measured raw signals into element mass fractions. Ensuring transparency in data processing, the results file (.xlsx) includes the calculated element mass fractions, associated statistical parameters as well as input data alongside instrument settings. Additionally, users can download a more comprehensive file containing the intermediate results of each calculation step. The software's key advantages include implemented corrections for isobaric interferences and abundance sensitivity.

The capabilities of G.O.Joe are demonstrated through the processing of two case studies, including trace element analyses of tungstates (e.g., scheelite) and silicates (e.g., garnet). In conclusion, G.O.Joe is a time-efficient, transparent and easy-to-use software tool that appeals to both experienced LA-ICP-MS users as well as newcomers to LA-ICP-MS data analysis. More details and the latest version of G.O.Joe are available at the following link: <https://www.gojoe.software>

References

Altenberger, F., Krause, J., Auer, T., Auer, A. Berndt, J (2024). *Geostandards and Geoanalytical Research.*, 49, 2, p. 281-294

The eastern Ruhla Crystalline Complex: Evidence for multi-directional deformation

Georg Löwe¹ and Peter Hallas¹

¹ *Thüringer Landesamt für Umwelt, Bergbau und Naturschutz, georg.loewe@tlubn.thueringen.de*

The Ruhla Crystalline Complex (RCC) is located in the northwestern Thüringer Wald and represents a complex assemblage of metamorphic rocks that form part of the NE-trending Mid-German Crystalline Zone (MGCZ). The MGCZ separates the Saxothuringian and the Rhenohercynian zones of the central European Variscides and is interpreted to represent a suture between the crustal units of Avalonia and Gondwana. The RCC represents a metamorphic nappe-stack, comprising the Liebenstein-, Brotterode-, Truse- and Ruhla units, which were emplaced during the Variscan orogeny (Zeh, 1996; Zeh et al., 2000). Although the geodynamic framework is rather well constrained, the structural inventory of the RCC paints a more complex picture.

We present geochemical, structural and thermobarometric data of samples from the southeastern RCC, namely the Brotterode- Truse- and Liebenstein units. Whole-rock geochemical data suggests three distinct types of protoliths, which are felsic- and basic igneous rocks and sedimentary rocks. Thermobarometric modelling of pseudosections indicate maximum metamorphic conditions of up to 800°C and 6-7.5 kbar for gneisses of the Brotterode unit and 650-750°C and up to 8 kbar for metamorphic rocks of the southern Truse unit, which are in good agreement with previously published data.

Mica schists of the Brotterode unit display a SE/E-dipping foliation and shear-sense indicators in thin section such as c'-type shear bands and Grt-sigma clasts imply top-NE transport. Elevated metamorphic conditions within the Truse unit result in small-scale folding with NE-plunging fold axes. Larger folds are NE-trending and result in the folding of the main foliation.

References

- Zeh, A. (1996). Die Druck-Temperatur-Deformations-Entwicklung des-Ruhlaer Kristallins (Mitteldeutsche Kristallinzone). Geotektonische Forschungen 86, Schweizerbart'sche Verlagsbuchhandlung, 212p.
- Zeh, A., Cosca, M. A., Brätz, H., Okrusch, M., & Tichomirowa, M. (2000). Simultaneous horst-basin formation and magmatism during Late Variscan transtension: evidence from 40Ar/39Ar and 207Pb/206Pb geochronology in the Ruhla Crystalline Complex. *International Journal of Earth Sciences*, 89(1), 52-71.

Trace element distribution in sulfides of the Kupferschiefer-Type mineralization, Röhrigschacht Wettelrode (Saxony-Anhalt)

Christian Lohmann¹, Nico Kropp¹, Ralf Halama¹, Harilaos Tsikos¹, and Michael Stipp¹

¹ *Martin-Luther-University Halle-Wittenberg, christian.lohmann@geo.uni-halle.de*

The Kupferschiefer-type mineralization of the Southern Permian Basin in Poland and Germany constitutes the largest base-metal resource in Europe. Despite decades of research, key scientific questions remain unresolved, particularly regarding the spatial distribution of metals within individual deposits and the mineralogical host phases of economically relevant trace elements (e.g., Ag, Se, Cd, V). The latter have been historically exploited and continue to contribute to the economic significance of the mineralization.

This study focuses on samples from Kupferschiefer-type mineralization hosted by Rotliegend sandstones, the basal Zechstein black shale (T1), and overlying Zechstein carbonates. The three lithotypes were systematically sampled along vertical profiles exposed underground at the Röhrigschacht in the Sangerhausen mining district. Thin sections were analyzed by μ XRF in order to generate element distribution maps. Mineral assemblages and ore textures were characterized using reflected-light microscopy as well as scanning electron microscopy using backscattered electron (BSE) imaging, and energy-dispersive spectroscopy (EDS). Trace element concentrations in sulfides were quantified by electron probe microanalysis (EPMA).

The results confirm the classical vertical base-metal zoning pattern characteristic of the Sangerhausen district, with a Cu–Pb–Zn sequence from bottom to top. However, locally anomalous element distributions were also identified, deviating from the expected zoning trends. Selenium was detected in nearly all sulfide phases (up to 0.26 at%). Silver occurs in sphalerite (up to 0.02 at%), chalcopyrite (up to 0.02 at%), bornite (up to 0.05 at%), and galena (up to 0.07 at%). Furthermore, the presence of mineralized fault structures and evidence of brittle–ductile deformation in ore minerals indicate not only late mineralization, but also post-ore tectonic overprinting related to the Upper Cretaceous uplift of the Harz Mountains affecting the Wettelrode deposit. Hence, there is repeated overprinting of deformation and mineralization. Overall, these findings provide new insights into the mineralogical complexity and metallogenic evolution of Kupferschiefer-type mineralization.

Exhumation through Vertical Extrusion: A Modeling Study of the Rhodope Metamorphic Complex

Iskander A. Muldashev¹ and Thorsten J. Nagel¹

¹ Institut für Geologie, TU Bergakademie Freiberg, iskander.muldashev@geo.tu-freiberg.de

We explore the fate of subducted continental margins using thermomechanical modeling with constant-force boundary conditions. Under certain conditions, large volumes of upper crust can get subducted to mantle depth, detach from the slab, and rise through the upper plate's lithosphere even against considerable compressive tectonic stress. At the surface, such an event is expressed as a phase of intense horizontal extension and magmatism internal of the oceanic suture zone. The process can create normal-fault-bounded core complexes hundreds of kilometers wide, in which metamorphic continental crust derived from the subducting plate is exposed. Horizontal tectonic stress and the thickness of the downgoing upper crust control the width of complexes, their topographic elevation, and the subduction depth of exposed rocks. We propose that the Rhodope Metamorphic Complex on the Balkan Peninsula represents a prime example for such vertical extrusion internal of a suture zone. Lower tectonic units in this domain exhibit Eocene high-pressure metamorphism and nappe stacking followed by massive magmatism and large-offset normal faulting. Despite more than 100 km of extension in Cenozoic times, the area still has thick crust. Our modeling results support schemes that attribute the lower units of the Rhodope Metamorphic Complex to the subducted Adriatic plate.

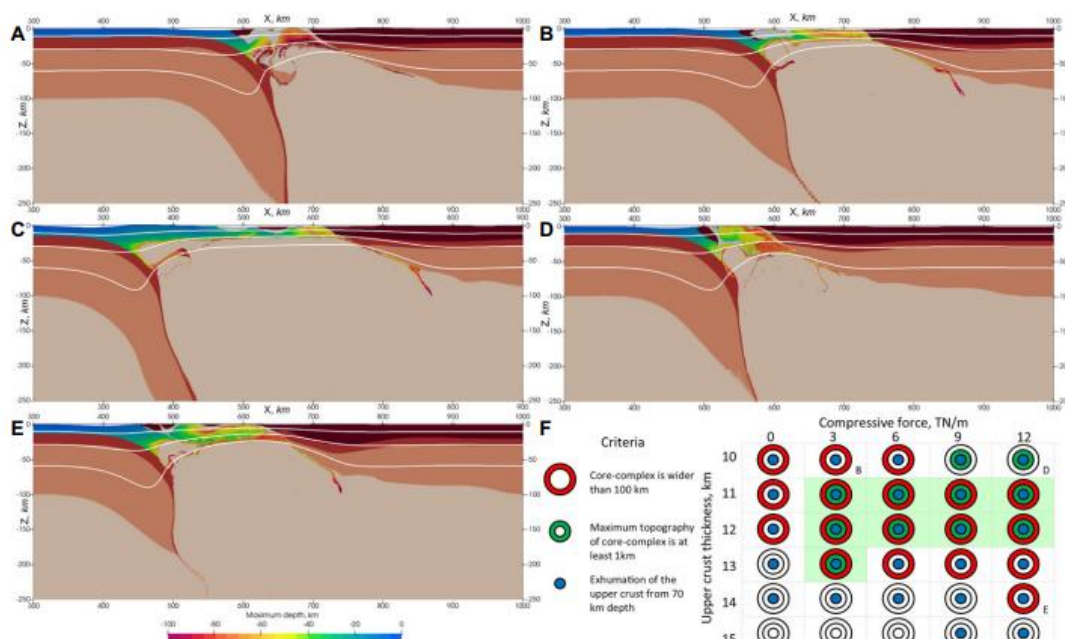


Figure 1. Final state of the model with (A) strong rheology of the upper crust; (B) thin crust and low compressive force; (C) thick crust and low compressive force; (D) thin crust and high compressive force; (E) thick crust and high compressive force. (F) Criteria table for the models with weak rheology of the crust (Ranalli, 1997). From Muldashev and Nagel, 2026.

Seismic velocity profiles, petrological velocity modeling and the architecture of the crust in Bulgaria

Thorsten Nagel¹, Gergana Georgieva², and Christian Schiffer³

¹ TU Bergakademie Freiberg, thorsten.nagel@geo.tu-freiberg.de

² Sofia University "Sv. Kliment Ohridski"

³ Uppsala University

We derive s-wave velocity profiles through the continental crust and the uppermost mantle in Bulgaria via joint inversion of receiver functions, p-wave polarization and ambient noise surface waves. In a next step we try to reproduce these profiles from the middle crust downwards through petrological velocity modeling along temperature gradients that are calculated for a layered lithosphere and constrained by surface heat flow. In this poster we illustrate the work flow of the second work phase: How we derive thermal gradients and mainly how we calculate velocities along corresponding temperature-pressure sections through phase diagrams. We show preliminary results for stations of the Adria-Array network in Bulgaria. Lower crustal velocities are often best reproduced by wet mafic compositions. For many stations, our present inversion scheme predicts a sub-Moho layer in the uppermost mantle, which is defined by varying thickness and a transitional lower boundary towards typical mantle velocities. Velocities in this layer are somewhat varying and in between velocities for crustal and mantle rocks. A possible explanation for this layer could be the presence of small amounts of hydrous phases in the uppermost lithospheric mantle.

Operando 4D synchrotron tomography reveals transport-controlled multiphase dolomitization in natural carbonate rock

Ng, Arthur¹, Nick Harpers¹, Andrew King², and Florian Fuisseis¹

¹ ASG, RWTH-Aachen University / a.ng@asg.rwth-aachen.de

² PSICHÉ beamline, Synchrotron SOLEIL, France

Dolomitization of carbonates generates ~12.9% additional porosity because dolomite has a smaller molar volume than calcite. The process can thus restructure pore networks in tight carbonate reservoirs, which improves and preserves storage capacity, permeability, and fluid connectivity at depth¹. Consequently, quantifying the kinetics, spatial distribution, and transport controls of dolomitization is essential for understanding and exploiting its economic and energy resource potential. Although reaction rate laws have been experimentally constrained², existing approaches cannot directly quantify the coupling between transport geometry, microstructural evolution, and replacement kinetics, nor determine whether dolomitization under advective conditions follows transport-limited scaling predicted by reactive transport theory.

Here, we present early analyses of operando (4D) μ CT data acquired at the PSICHÉ beamline, Synchrotron SOLEIL, documenting hydrothermal dolomitization in fractured limestone from the Lower Carboniferous Kohlenkalk sequence (NRW, Germany). Experiments were conducted using the X-ray transparent Heitt Mjölñir triaxial flow-through rig³, with continuous injection of a 2.05 M NaCl–MgCl₂–CaCl₂ brine at 1.5 μ L min⁻¹, at 260 °C, 20 MPa confining pressure, and 15 MPa pore pressure. Reaction progress was resolved in 62 μ CT volumes at 5.8 μ m voxel size over 128 h, complemented by ICP-OES fluid analyses to track bulk mineralogical evolution and post-mortem SEM/EDX to confirm the stoichiometry of the reaction products, as well as sub-micron structures.

Our 4D μ CT data resolve the dolomitization process in space and time, allowing direct quantification of local reaction rates of the coupled reactions, and transport regimes: Calcite reacts with the brine to form magnesite, dolomite, and locally brucite. Magnesite and brucite remain largely confined to inlet regions, whereas dolomite nucleates preferentially along hydraulically active fractures and stylolites with apertures >32 μ m. Magnesite precipitation generates macro-porosity (10–100 μ m) that enhances advective flow, while dolomite-type replacement produces sub-micron porosity consistent with diffusion-dominated transport. These observations demonstrate strong chemical-hydraulic feedbacks that produce spatially heterogeneous transport regimes and control overall replacement kinetics. Our data uniquely reveal the non-linear acceleration of reaction front propagation and how they are coupled with evolving transport pathways, providing a mechanistic basis for scaling dolomitization to natural hydrothermal systems.

References

¹Warren, J. (2000). doi.org/10.1016/S0012-8252(00)00022-2

²Arvidson & Mackenzie (1999). <https://doi.org/10.2475/ajs.299.4.257>

³Freitas et al. (2024). <https://doi.org/10.1107/S1600577523009876>

Influence of initial grain size on quartz deformation and static recovery

Malte Ortmanns^{1,2}, Petar Pongrac¹, Petr Jerabek³, Sebastian Cionoiu¹, Jean Furstoss⁴, Yuval Boneh⁵, and Lucie Tajcmanova¹

¹ Heidelberg University

² MLU Halle-Wittenberg, malte.ortmanns@geo.uni-halle.de

³ CU Prague

⁴ University of Poitiers

⁵ Ben Gurion University of the Negev

In this study, we performed deformation experiments on encapsulated powdered samples from a crushed single quartz crystal, with grain size ranges of 1) 64-125 μm , 2) 20-64 μm and 3) <20 μm . The experiments were performed using a Griggs-type solid-medium apparatus, in pure shear setup, under conditions of 1 GPa, 900 °C, achieving strain rates of 10⁻⁶ s⁻¹, and with 0.1 wt% of added H₂O.

Samples were investigated by light microscopy and EBSD analysis. A hot-pressed sample of the large fraction showed a progressive recovery microstructure, where relatively smaller grains, with initially low internal misorientation, grew at the expense of larger, more strained grains, while the total grain boundary density remained constant throughout the microstructural evolution. Contrary to conventional grain growth models, this indicates that local differences in stored strain energy can dominate static grain growth, overriding surface energy as the primary driving force. Samples deformed in pure shear setup have shown contrasting strain localization and different microstructural evolution with respect to the thermal gradient, with the maximum temperature at the middle parts of the samples. The large fraction showed a progressive strain localization following the thermal gradient, associated with increasing degree of SGR-type of recrystallization. In contrast, the middle fraction showed a regressive strain localization with respect to the thermal gradient, followed by microstructural shift from SGR-dominated to GBM-dominated recrystallization. The resulting strain rate partitioning was followed by opening wide Mode I cracks in the slow strain rate GBM-region due to tensile drag forces exerted by the fast strain rate SGR-parts. The small fraction showed an interplay between GBM, subgrain rotation, and strain-driven grain growth. Here, the differential stresses below 100 MPa allowed for grain-recycling set of processes:

- 1) initial migration of grain boundaries and annihilation of most of very fine grains,
- 2) slow development of subgrains and their detachment as new strain-free grains,
- 3) strain energy induced growth of new strain-free grains at the expense of larger more strained grains,
- 4) straining of the growing grains and their repeated recrystallization.

References

Pongrac, P., Ortmanns, M., Jeřábek, P., Cionoiu, S., Furstoss, J., Boneh, Y., Tajcmanová, L., 2026. Strain energy-driven grain growth in quartz aggregates: Implications for microstructural evolution and recovery. *Tectonophysics* 918, 230971. <https://doi.org/10.1016/j.tecto.2025.230971>

Ar-Ar geochronology I - Applications, limitations, developments and future improvements

Jörg A. Pfänder¹, Blanka Sperner¹, and Thorsten Nagel¹

¹ *Institut für Geologie, TU Bergakademie Freiberg, pfaender@tu-freiberg.de*

Along with the U-Pb dating method, Ar-Ar dating is one of the most powerful geochronometers in Earth Sciences, capable of dating a variety of K-bearing minerals and rocks. Due to the high mobility (diffusivity) of argon in minerals, Ar-Ar ages are other than U-Pb ages mostly cooling ages, i.e., mark the time in the past when a specific mineral species passed through a distinct temperature range during cooling. As such they are powerful tools not only for dating e.g., volcanic eruptions, but also for reconstructing the thermal histories of rocks. One of the most striking improvements in Ar-Ar geochronology over the last two decades was the technical improvement of noble gas mass spectrometry. The machines became successively more sensitive, more precise and more accurate. This challenged the type of material that can be reasonably well dated, as natural minerals are complex systems down to the atomic scale. Therefore, the new equipment often does not provide more accurate ages but reveals the complexity of natural material (the so-called overdispersion; see Schaen et al., 2020, for a review). In addition, uncertainties imprinted on Ar-Ar ages during irradiation by neutron fluence gradients that can be in the order of up to a few percent, or the necessary correction of nucleogenic isobaric interferences became even more significant. Nevertheless, the new high-precision instrumentation has great potential due to its high sensitivity and precision that allows for a reduced sample size, thus minimizing the drawbacks related to neutron irradiation and sample heterogeneity. Even step-heating experiments on small single grains are now possible, which results in better constrained age distributions in metamorphic and detrital rocks if compared to the single-grain total-fusion approach.

Any further improvement of instrumentation, however, will not necessarily lead to more accurate Ar-Ar ages from continuously smaller samples, as long as the problems of neutron fluence gradients and interfering argon isotope corrections (particularly for minerals with high Ca/K ratios such as amphiboles) are not solved. Even neglecting these, a system immanent physico-chemical limitation will always remain, namely the 'blank problem', which is the argon signal background that results from the desorption of argon from the inner surfaces of the instrumentation during measurement. This 'blank' cannot be properly quantified and thus defines the unshiftable lower limit of the detectable signal and thus of the size (spot) of a sample.

Future improvements in Ar-Ar geochronology are not only related to a better instrumentation, but need to focus on a better knowledge of 'what' is dated before it is dated, i.e., on the physico-chemical characterization of the investigated phases (homogeneity, chemistry, crystal lattice state, inclusions, grain dimensions, ...). This hopefully will help to further improve our understanding of 'complex' data obtained from step heating experiments.

References

Schaen, A. J., Jicha, B. R., Hodges, K. V., Vermeesch, P., Stelten, M. E., Mercer, C. M., ... & Singer, B. S. (2021). Interpreting and reporting ⁴⁰Ar/³⁹Ar geochronologic data. *GSA Bulletin*, 133, 461-487.

Magmatic plumbing systems and their role in continental breakup - an example from Messum, Namibia

Jörg A. Pfänder¹, Philipp Holaschke¹, Joachim Krause², Andreas Klügel³, Thorsten Nagel¹, Stefan Jung⁴, and Carsten Münker⁵

¹ TU Bergakademie Freiberg, Institut für Geologie pfaender@tu-freiberg.de

² Helmholtz-Zentrum Dresden-Rossendorf, Helmholtz Institut Freiberg für Ressourcentechnologie

³ Universität Bremen, Fachbereich Geowissenschaften

⁴ Universität Hamburg, Institut für Mineralogie

⁵ Universität zu Köln, Institut für Geologie und Mineralogie

Numerous studies have evaluated the magmatic evolution and origin of extrusive magmatic rocks of large igneous provinces (LIPs), whose formation is commonly linked to mantle plumes and which are often assumed to assist or trigger rifting and subsequent continental breakup. Much less is known about the plumbing systems of LIPs, about magma transport rates, storage times and differentiation within the lithosphere, and about the volume and composition of their plutonic portion as part of the continental crust. This, however, is crucial in deciphering the local thermal state of the lithosphere and crust, which in turn is critical in determining its local rheological behaviour and response to crustal stresses prior to breakup. This study presents mineral and whole-rock geochemical and petrological data from different types of gabbros from Western Namibia, which are thought to represent the upper part of a deep reaching plumbing system that fed the Paranja-Etendeka LIP ~132 Ma ago. Magmatism at this time broadly coincides with the breakup of Western Gondwana and the opening of the South Atlantic Ocean.

Major- and trace element systematics and thermodynamic modelling suggest that the gabbro parental magma(s) developed from a tholeiitic picritic melt with up to 18wt% MgO by >10% olivine fractionation. The picritic primary magma was formed by ~14% partial mantle melting. Liquidus temperatures have been as high as ~1525°C (3 GPa) and mantle potential temperatures in the order of 1455-1470°C, significantly higher than estimates for the convecting mantle (1280-1340°C) but consistent with estimates assigned to the Tristan mantle plume head upon impacting the Gondwana lithosphere (Gibson et al., 2005). Clinopyroxene trace element data are inconsistent with gabbro formation by pure fractional crystallization from a common magma, but in support of substantial assimilation of Pan-African continental crust accompanied by high crystallization rates. These observations imply intense heat exchange between the plumbing system and ambient crust, which possibly led to marked local heating and crustal weakening.

References

Gibson, S.A., Thompson, R.N., Day, J.A., Humphries, S.E., Dickin, A.P., 2005, Melt-generation processes associated with the Tristan mantle plume: Constraints on the origin of EM-1. *Earth Planet. Sci. Lett.*, 237, 744-767.

Poly-metamorphic evolution of a slice of the Briançonnais terrane: structural and petrographic evidence from the Tambo Nappe (Central Alps)

Enrico Pigazzi¹, Francesco Arrigoni², Leo J. Millonig⁴, Filippo L. Schenker³, Axel Gerdes⁴, Paola Tartarotti², and Lucie Tajčmanová¹

¹ Heidelberg University, Institute of Earth Sciences enrico.pigazzi@geow.uni-heidelberg.de

² University of Milan (UNIMI), Earth Sciences Department "A. Desio"

³ University of Applied Sciences and Arts of Southern Switzerland (SUPSI), Institute of Earth Sciences

⁴ FIERCE (Frankfurt Isotope and Element Research Center), Goethe University Frankfurt, Institute of Geosciences

The study of the crystalline basement nappes of the Briançonnais Domain provides not only insights into the mechanisms responsible for the Alpine orogeny but also into the pre-Alpine geodynamic evolution of the southernmost portion of the paleo-European plate.

Situated at the north-eastern margin of the Lepontine Dome, the Tambo Nappe represents a clear example of poly-metamorphic basement characterized by a long-lasting and intricate tectonic history. Given the widespread preservation of pre-Alpine textures and mineral associations, detailed analysis of their relationships with the Alpine mineral parageneses and structures provides valuable constraints for deciphering the complex geological evolution of the entire nappe.

In light of the outcome of the new Swiss and Italian National geological maps of this sector of the Alps, petrographic and structural evidence are presented that point to a regional medium- to high-temperature metamorphic event predating the Alpine overprint, possibly chronologically associated with the previously recognized Permian magmatism in this region.

These findings are discussed in terms of their geological and geodynamic significance within the broader geodynamic framework of the adjacent nappes in the Central Alps, also highlighting the uncertainties arising from different interpretations which require further petro-chronological studies to be clarified.

Do quartz-in-garnet Raman spectroscopic data and garnet fabrics reveal a fluid infiltration event in the south of the Adula nappe?

Jan Pleuger¹, Xin Zhong¹, Olga Brunsmann¹, Kristina G. Dunkel², Marisa Germer¹, Vincent Könemann¹, Victoria Kohn³, Luca Menegon², Guyu Peng⁴, Alexandra Pohl¹, Julien Reynes⁵, and Timm John¹

¹ *Institute of Geological Sciences, FU Berlin, jan.pleuger@fu-berlin.de*

² *The Njord centre, Department of Geosciences, University of Oslo*

³ *Naturhistorisches Museum Wien*

⁴ *Department of Environmental Analytical Chemistry, Helmholtz Centre for Environmental Research, UFZ Leipzig*

⁵ *Institute of Earth Sciences, University of Lausanne*

The Adula nappe in the Swiss-Italian Alps consists of alternating orthogneiss and metasediment-rich subnappes, the latter of which host eclogite and garnet peridotite lenses. Peak pressures and concomitant temperatures determined on eclogites and garnet peridotites define gradients from ~ 1.5 GPa/ ~ 500 °C in the north to ~ 3 GPa/ ~ 750 °C in the south (see compilation of pressure-temperature paths in Nagel 2008). Contrary to the (ultra-)basic lenses, eclogite-facies assemblages have been reported from only very few localities and commonly show a strong Barrowian overprint. We studied more than 50 samples from all garnet-bearing lithologies using quartz-in-garnet Raman elastic barometry and Zr-in-rutile Thermometry. Our aim is to reappraise the north-south pressure and temperature gradients, respectively.

The temperature values increase steadily from ~ 500 °C in the north to ~ 700 °C in the south of the nappe. The entrapment pressures of quartz inclusions in garnet record a sharp drop from up to ~ 2.3 GPa in the north and middle to ~ 1.0 GPa in the south. The chemical zonations of garnet and modal percentages of hydrous minerals as a proxy for fluid availability show that with higher water content in the bulk rock and at higher temperatures, quartz inclusion pressures tend to be mechanically reset to lower pressures. This is corroborated by Fourier-transform infrared spectroscopy data showing that garnet from the south of the nappe typically contains structural water or submicroscopically small amounts of hydrous phases. We suggest that chemical homogenisation of garnet and resetting of quartz inclusions in the south of the nappe may be due to nappe-scale fluid infiltration during retrograde metamorphism under low-pressure, but still (near) peak-temperature conditions.

References

Nagel, T.J. (2008): Tertiary subduction, collision and exhumation recorded in the Adula Nappe, central Alps. In: Siegesmund, S., Fügenschuh, B. & Frotzheim, N. (eds.): Tectonic aspects of the Alpine-Dinaride-Carpathian System. Geological Society, London, Special Publications 298, 365-392.

Microanalysis of Shock Experiments on K-Feldspar

Michael H. Poelchau¹, Dominic Wölki¹, and Thomas Kenkmann¹

¹Freiburg University, michael.poelchau@geologie.uni-freiburg.de

The confirmation of impact structures on earth relies mainly on the identification of diagnostic microstructural features in minerals deformed by the passage of the shock wave. While these features are well described in quartz, work on other minerals remains lacking. In fact, according to Cavosie et al. (2024), only shock features in quartz are accepted as proof for shock metamorphism in impact craters. We intend to improve this situation and document the range of shock features found in other common minerals, particularly feldspars. Here we focus on K-feldspar.

Two plane wave shock recovery experiments that were performed in 1999 at the Ernst Mach Institute in Weil am Rhein, Germany, were reanalyzed. A high explosive-driven flyer plate impacted a cylindrical ARMCO-Fe container and cylindrical sample (15 mm diameter, 10 mm thick), which was composed of a vertical quartz-K-feldspar-quartz sandwich (cf. Kenkmann et al., 2000). Calculated peak pressures were 25 and 16 GPa in quartz at the upper interface to the iron container and receded to an estimated pressure of 5–6 GPa at the base of the sample.

SEM analysis of K-feldspar shows localized patches of twins with μm to sub- μm spacing, which are easily recognized by narrowly spaced alternating cleavage patterns (Fig. 1a). Planar deformation features (“PDFs”, i.e., amorphous lamellae) are common in quartz as darker, lower density bands but are more difficult to image in feldspar (Fig. 1b). In general, PDFs are much less pervasive in K-feldspar compared to quartz, and feldspar twins show an uneven distribution. Mapping is planned to constrain twin and PDF occurrence relative to decreasing pressures and mineral interfaces, and to reveal possible fluctuations in bulk and differential pressures during the passage of the shock wave.

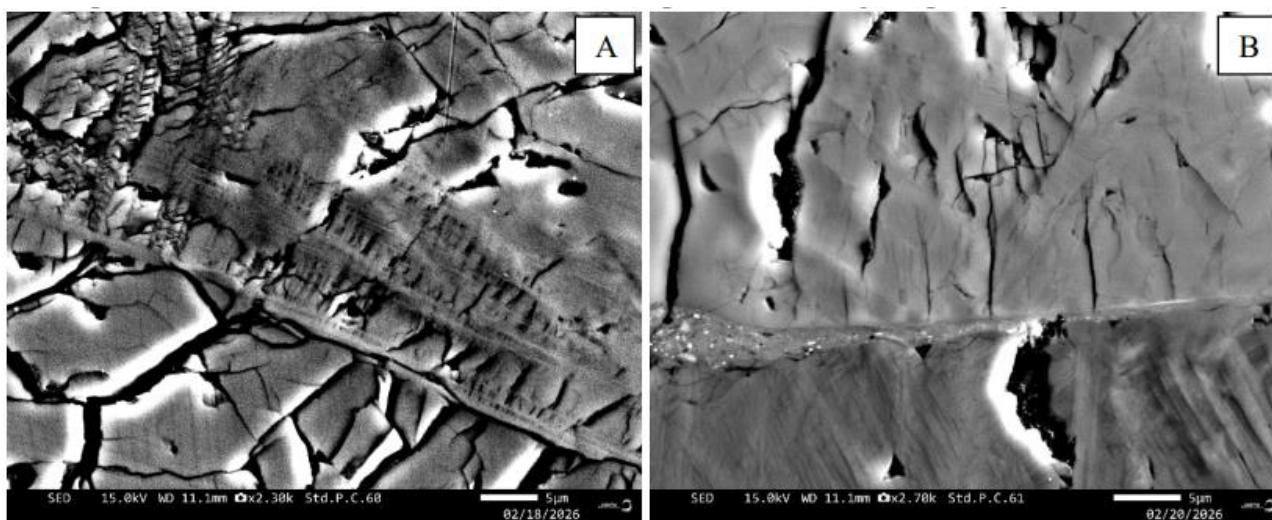


Figure 1. A) μm -scale twinning in Kfsp can be seen in the upper left. In the center, what appears to be glassy lamellae run WNW-ESE. In the lower left, subtle darker lamellae are assumed to be PDFs. B) PDFs are more easily seen in quartz (bottom) than Kfsp. Localized melting occurs at the contact.

References:

- Kenkmann, T., U. Hornemann, and D. Stöffler (2000), Experimental generation of shock-induced pseudotachylites along lithological interfaces, *Meteorit. Planet. Sci.*, 35, 1275–1290.
 Cavosie, A. J. et al. (2024). A Diagnostic Impact Criteria List to Confirm Terrestrial Impact Craters by the MetSoc Impact Cratering Committee—Work in Progress. In 86th MetSoc (Vol. 86, No. 3036, p. 6248).

The Paku Tin Deposit: A Deformed Greisen Mineralization?

Nimatul Azizah Raharjanti¹, Joachim Krause¹, Arifudin Idrus², Ernowo³, Wahyu Vian Pratama⁴, and Jens Gutzmer¹

¹ *Helmholtz-Zentrum Dresden-Rossendorf, Helmholtz Institute Freiberg for Resource Technology, Freiberg, Germany, n.raharjanti@hzdr.de*

² *Department of Geological Engineering, Universitas Gadjah Mada, Yogyakarta, Indonesia*

³ *National Research and Innovation Agency, Banten, Indonesia*

⁴ *PT Timah Tbk*

The Southeast Asian tin belt is the world's most important tin-producing region (Schwartz et al. 1995). An integral part of this tin belt is located in Indonesia, currently the world's second-largest tin producer, from both primary and secondary ore deposits. The Paku site on Bangka Island is one of the currently producing primary tin deposit. Tin mineralization at the Paku deposit has been divided into a near-surface oxide zone and a deeper sulfide zone. Little is known about the geological setting of this deposit in published literature, but mineralization is characterized by the occurrence of polymetallic veins and disseminated cassiterite mineralization (Jaya et al. 2019) that both cut steeply across a host rock succession of metamorphosed metasedimentary rocks.

The current investigation is based on a number of exploration drill core samples taken from this sulfide zone of the deposit, with the aim to characterize the style of mineralization and identify possible effects of hydrothermal alteration. Observations from the combination of with μ -XRF analysis of drill core surfaces with reflected-light microscopy and SEM-based automated mineralogy (MLA) conducted on polished thin sections revealed the presence of at least three distinct paragenetic stages of mineralization that replace and crosscut the metamorphic host rock. The first stage is marked by the occurrence of idiomorphic cassiterite associated with an assemblage of quartz, muscovite, topaz, and minor fluorite and rutile. This assemblage replaces the metasedimentary host rock. The first stage is cross-cut by a polymetallic sulfide-rich assemblage occurring disseminated and/or veinlet-bound. This mineralization stage consists predominantly of pyrite, sphalerite, galena, chalcopyrite, and ferrokesterite, with minor arsenopyrite and pyrrhotite. The third stage relates to various degrees of supergene alteration, occurring as goethite, covellite, and cerussite.

Distinct cataclastic and mylonitic deformation structures are observed to affect the first two stages of mineralization. This suggests that intensive deformation postdates hydrothermal ore formation. Although strike-slip faults have been mapped in the area (Jaya et al. 2019), mechanisms responsible for the development of this deformed greisen-type mineralization remain poorly constrained. Further field studies are carried out to reveal the relation between intense deformation and mineralization. Exploration drill cores will be sampled more extensively to understand the nature of the host rock succession – and its relation to hydrothermal mineralization. This will be supported by mineral chemical and geochemical analyses in order to place constraints on the mineralization processes at the Paku deposit in order to link this to the regional geotectonic evolution (Barber et al. 2005) and to other deposits of the Southeast Asian tin belt (Schwartz et al. 1995).

References

- Barber AJ, Crow MJ, Milsom J (eds) (2005) *Sumatra: geology, resources and tectonic evolution*. The Geological Society, London
- Jaya RAF, Artyanto A, Pasemah AS (2019) Characterization of Primary Sulfide Tin Deposits Paku Area, South Bangka, Indonesia. In: MGEI PROCEEDINGS. Bogor, Indonesia
- Schwartz MO, Rajah SS, Askury AK, et al (1995) The Southeast Asian tin belt. *Earth-Science Reviews* 38:95–293. [https://doi.org/10.1016/0012-8252\(95\)00004-T](https://doi.org/10.1016/0012-8252(95)00004-T)

Serpentinization of orthopyroxene in oceanic serpentinites

Marie C. Reichardt¹ and Rebecca Kühn¹

¹ *Martin-Luther-Universität Halle-Wittenberg*

The Atlantis Massif is an oceanic core complex at the slow spreading mid-Atlantic ridge. Due to insufficient melt supply, serpentinized mantle peridotites are exhumed along a large detachment fault. A ~1.2 km deep hole was drilled into the footwall of this detachment fault during IODP Expedition 399. Most of the recovered serpentinites have a harzburgitic protolith. Orthopyroxene reaction progress ranges from almost unaltered to fully serpentinized, often forming complex core-rim structures at the grain scale. Reaction rims appear to have variable thickness in different directions. Here, we explore whether a general preferential direction of pyroxene serpentinization with respect to a geographic reference frame exists by means of image analysis of full thin section μ XRF maps. The thickness of the alteration rims was measured as a function of its normal direction and corresponds to the distance between the boundary pyroxene core – serpentinized pyroxene area and the outer rim of the alteration phase.

In general, the grain size distribution of orthopyroxenes has a mode of ~1.5 mm equivalent diameter. The aspect ratios of the pyroxenes range between 1 and 4.2 with a mode of ~1.5. The majority of grain long axes is subperpendicular to the drill core axis. Serpentinized orthopyroxene grains within each investigated sample show a preferred direction of higher reaction progress, irrespective of the grain shape anisotropy. This preferred orientation is especially prominent in incompletely serpentinized samples.

When we compare the overall direction of the preferential serpentinization, we observe the largest extent of reaction rims in the direction parallel to the drill core axis, which is also perpendicular or subperpendicular to a preferred orientation of magnetite aggregates, often suspected to trace initial fluid pathways.

Whether the preferential serpentinization direction of orthopyroxene is determined by fluid availability or by the direction of largest normal stress, will be discussed.

Microstructural evidence of tectonic overpressure.

Anna Rogowitz¹, Philippe Goncalves² Bernhard Grasemann³, Zhaoliang Hou⁴, and A. Hugh N. Rice³

¹ *Department of Geology, University of Innsbruck, Innsbruck, Austria,*
anna.rogowitz@uibk.ac.at

² *Laboratoire Chrono-environment, University of Franche-Comté*

³ *Department of Geology, University of Vienna, Vienna 1090, Austria*

⁴ *State Key Laboratory of Geological Processes and Mineral Resources, Frontiers Science Center for Deep-time Digital Earth, China University of Geosciences*

Stable mineral assemblages are commonly interpreted to record equilibration under isotropic stress, with pressure reflecting the lithostatic load and peak-pressure assemblages indicating maximum burial depth. However, numerical models predict that viscous deformation in mechanically heterogeneous rocks can generate localized deviations from lithostatic pressure, referred to as tectonic overpressure. Whether such tectonic overpressures are preserved in natural rocks remains debated.

We present microstructural and mineralogical evidence for tectonic overpressure preserved in a sheared biotite schist forming a discrete ~1.5 cm-thick high-strain layer. The schist is composed of biotite, epidote, sphene, quartz, and garnet, with accessory apatite and white mica. Pervasive kinematic indicators (SCC' fabrics, δ -clasts, sigmoids) record top-to-the-SE shear. Additional kinematic constraints come from the SPO of sphene, inclined ~ 30° to the main foliation opposite to the shear sense, and from aligned white mica aggregates concentrated in compressional quadrants around rigid clasts (epidote, sphene, garnet, apatite).

Thermodynamic modelling indicates that the equilibrium assemblage (biotite–sphene–garnet–epidote–quartz) is stable across ~6.2–8.2 kbar and 510–680 °C. In contrast, white mica in compressional quadrants of clasts has a phengitic, high-pressure composition implying ≥ 10 kbar. The coexistence of these contrasting pressure estimates at thin-section scale challenges the assumption that mineral assemblages record lithostatic pressure.

Spinel-bearing cumulate dunite in garnet-bearing ultramafic rocks of Zöblitz (Erzgebirge) - Implications for the pre-subduction evolution of mantle-derived ultramafic rocks in the Erzgebirge UHP terrane

Kilean Rohr¹, Joachim Krause², Jörg A. Pfänder³, Sabine Gilbricht³, and Stefan Jung⁴

¹ Georg-August-Universität Göttingen, kileanfelix.rohr@stud.uni-goettingen.de

² Helmholtz-Zentrum Dresden-Rossendorf, Helmholtz-Institut Freiberg für Ressourcentechnologie

³ TU Bergakademie Freiberg

⁴ Universität Hamburg

Ultramafic rocks derived from the subcontinental or suboceanic mantle provide valuable information on the composition and evolution processes of this part of the silicate Earth (Bodinier & Godard, 2003). This study focuses on lithologies associated with the garnet peridotite of Zöblitz, which is part of the UHP-HT Gneiss-Eclogite Unit of the Erzgebirge. Petrographic investigations, particularly serpentine textures, indicate that one of the sampled lithologies represents a serpentinized spinel-bearing dunite. Primary spinel grains preserved as inclusions in former olivine grains exhibit compositional zoning characterized by increasing Cr and decreasing Al contents from core to rim, suggesting fractional crystallization as the dominant formation process. This interpretation is supported by spinel compositional trends for Fe and Ti (Barnes & Roeder, 2001). Together with the absence of a preferred orientation of olivine grains, typical for residual dunites, a cumulate dunite is inferred. Interstitial spinel grains show compositions distinct from those of primary inclusion spinels with weak or absent zoning. These characteristics are interpreted as a result of reaction or recrystallization processes caused by percolating melts between the cumulus crystals. Many primary spinels recrystallized concomitant with klnochlore under amphibolite-facies conditions to form Al- and Mg-poor Cr-spinel with skeletal textures. Application of the spinel compositional fields for various rock types and tectonic settings identified by Barnes & Roeder (2001), combined with results from spinel investigations in the associated garnet peridotite and previous models by Schmädicke & Evans (1997) and Schmädicke & Will (2023), suggests that the dunite cumulate likely formed in a supra-subduction zone ophiolitic setting, with a spinel peridotite representing the precursor of the present garnet peridotite. Future work will focus on dating primary spinel to confirm its pre-subduction formation and on analyzing spinel trace element compositions to further constrain its mantle origin. These results will be evaluated in the context of the recent model of Kotková et al. (2025), which proposes the subcontinental lithospheric mantle as the source of the Erzgebirge garnet peridotite.

References

- Barnes, S. J., & Roeder, P. L. (2001). *J. Petrol.*, 42(12), 2279–2302.
 Bodinier, J.-L., & Godard, M. (2003). *Treatise on Geochemistry*, 2, 103–170.
 Kotková, J., Čopjaková, R., Kubeš, M., Ackerman, L., Sláma, J., Schmädicke, E., & Holá, M. (2025). *Lithos*, 516–517, 108234.
 Schmädicke, E., & Will, T. M. (2023). *J. Metamorph. Geol.*, 1–23.

The Miocene tectonic evolution of the western Tauern Window (European Alps): A spatial-temporal restoration

Julia Rudmann^{1,2*}, David C. Tanner¹, Hannah Pomella³, Christian Brandes⁴, Paul Eizenhöfer⁵, and Michael Stipp²

¹ *LIAG Institute for Applied Geophysics, Germany, julia.rudmann@gmx.de*

² *Martin Luther University Halle-Wittenberg, Germany*

³ *University of Innsbruck, Austria*

⁴ *Leibniz University Hannover, Germany*

⁵ *University of Glasgow, Scotland*

**now at State Authority for Mining, Energy and Geology – Lower Saxony, Germany*

The Tauern Window (TW) exposes nappes of the European Alpine orogenic wedge at the surface. These nappes were formed during the collision of the European plate with the Adriatic plate and then stacked in the Late Eocene. During the Miocene, the northward moving Dolomites indenter caused strong N—S-shortening and coeval W—E-extension at its front. This deformation phase overprinted the TW nappes and, ultimately, led to their exhumation. The western TW was modified the most, because N—S-shortening was strongest in this area. It is therefore a key area to understand the latest tectonic history of the Eastern Alps.

After the restoration of two N—S cross-sections (near the Brenner Base Tunnel and the TRANSALP seismic section) focusing on the core of the western TW (Venediger duplex), we interpolated 3-D surfaces across both cross-sections for each timestep, leading to a time-resolved restoration. Employing the software Move™, we constrained our models using published fission-track, P-T-t and geophysical data (e.g., seismic tomography). Between 23 – 17 Ma, shortening was accommodated by upright folding of the Venediger duplex. Area conservation reveals that W—E extension did not significantly affect the Venediger duplex. In contrast, its hanging-wall nappes experienced strong tectonic thinning, hence, strain partitioning. Between 18 – 17 Ma, the Dolomites indenter's middle/lower crust detached near the TRANSALP seismic section, causing heterogeneous deformation of the Venediger duplex. Within this timespan, folding gradually decreased from the top down, ceasing first at the top, as it entered progressively the brittle regime. From 17 Ma onwards, deformation transitioned to northward displacement of the Venediger duplex along the Sub-Tauern ramp. Additionally, within the last 10 Ma, the upper three nappes of the Venediger duplex thrust northward along the Sub-Ahorn ramp in the vicinity of the TRANSALP seismic section. Finally, our 4-D restoration reveals that Miocene indentation was multi-directional.

(Micro-) tectonics of tin bearing metasedimentary rocks of the Erzgebirge

Owishi Sarkar¹, Ida Hemplen², Uwe Kroner², Claus Legler³, and Rolf L. Romer¹

¹ *GFZ Helmholtz Centre for Geosciences, Telegrafenberg, D-14473 Potsdam, Germany, osarkar@gfz.de*

² *Department of Geology, TU Bergakademie Freiberg, B.-v.-Cotta-Strasse 2, D-09599 Freiberg, Germany*

³ *Freiberg, Germany*

Metasedimentary rocks in the Erzgebirge, northern margin of the Bohemian Massif (Central European Variscides), contain metamorphic cassiterite. The cassiterite formed at ca. 395 Ma and ca. 365 Ma [1] during a prograde and a retrograde regional metamorphic stage, respectively [2]. Tin was added along with SiO₂ in the prograde stage. It is present as elevated Sn contents in prograde biotite, as cassiterite disseminations in biotite-rich bands and along margins of quartz layers, and locally as inclusions in garnet porphyroblasts. The later stage of Sn mobilization is related to the retrogression of biotite which released Sn that was sequestered as fine cassiterite grains and as inclusions within chloritized biotite [3]. Here we present first results of microtectonic investigations of the Sn-bearing phyllites and mica schists generally characterized by recumbent folds that are obliterated by a pervasive foliation. The main characteristic of cassiterite and garnet bearing biotite layers is the static recrystallization of biotite. In contrast, the main foliation is characterized by strongly foliated layers of retrograde chlorite and muscovite in combination with massive quartz. As obvious from cm-scale relics of quartz grains, the fine-grained quartz fabric developed by dynamic recrystallization due to subgrain-polygonization and -rotation (SGR). Higher temperatures are indicated by contemporaneous dynamic recrystallization by grain boundary migration (GBM). Cassiterite crystallized along the outer margin of folded quartz layers and in pressure shadows of porphyroclasts. We interpret that micro-fabric of the Sn-bearing metasedimentary rocks is the result of polyphase interaction between synkinematic emplaced quartz veins and pervasive deformation during the prograde and the retrograde stage. The prograde and the retrograde evolution are not the result of a continuous burial-exhumation process, but represent two discrete stages of prolonged subduction accretion tectonics.

References

[1] Romer, R. L., Kroner, U., Schmidt, C., Legler, C., 2022. Mobilization of tin during continental subduction-accretion processes. *Geology*, 50, 1361-1365.

[2] Weber, S., Legler, C., Kallmeier, E., Schulz, B., Burisch, M., 2023. Metamorphic origin of stratiform cassiterite mineralization in the Schwarzenberg -Aue district – Clues to the metamorphic history and pre-orogenic Sn enrichment of the Erzgebirge (Germany). *Lithos*, 454–455, 107273.

[3] Sarkar, O., Romer, R. L., Kroner, U., and Legler, C., 2025. Mobilization of tin during metamorphism in the Variscan Orogeny. *EGU General Assembly 2025*, EGU25-6784, Vienna, Austria.

Magnetite microstructure in oceanic serpentinites

Luisa Schlickum¹, Rüdiger Kilian¹, and Rebecca Kühn¹

¹ *Martin-Luther-University Halle-Wittenberg*

Magnetite forms as a consequence of low-temperature serpentinization of ultramafic rocks, and is hence a common mineral in serpentinites at mid-ocean ridge oceanic core complexes. The observed serpentinite microstructure is typically assumed to be the result of the serpentinization process.

The Atlantis Massif is such an oceanic core complex where a ~1.25 km long section (U1601C) was drilled during IODP Expedition 399. Macroscopically, samples exhibit a variably strong magnetite foliation, ranging from fully dispersed to parallel, layer-like aggregates. Hence, we aim to understand if these different magnetite distributions form during the serpentinization reaction or if they are the manifestation of deformation processes. We address this question by analyzing microstructural parameters of magnetite based on EBSD, EDX and μ XRF data. Samples were chosen based on different types of magnetite distributions, i.e., spatially dispersed, in single-grain thick layers or in 3-dimensionally connected aggregates.

Modal grain sizes vary between 3 and 10 μ m equivalent diameter in all samples with the smallest grain size in samples with distributed magnetite. Long axes of individual grains within elongated, polycrystalline aggregates tend to be at a large angle to the long axes of the entire aggregate. Magnetite CPO is usually a well defined bimodal distribution; the misorientation between the two modes represents approximately a stacking fault-related twinning in magnetite (60° around $\langle 111 \rangle$). This twinning type can be related to growth or deformation twinning. Variations of the preferred alignment of low angle boundary traces as well as the preferred alignment of misorientation axes, hint towards a mechanism which modifies grain boundary directions as well as crystal misorientations between grains.

The relation between different types of magnetite distribution and the observed microstructural parameters will be discussed with regard to the development of the structures and possible mechanisms and processes leading to their formation.

Triaxial testing on rock salt in the context of hydrogen storage in caverns

Friedrich Schlosser¹, Florian Fritz¹, Rüdiger Kilian¹, André Eschenröder¹,
and Michael Stipp¹

¹ *Martin-Luther-Universität Halle-Wittenberg*

In the context of energy transition in Germany hydrogen is proposed as a replacement for fossil industrial gas. Since Germany lacks the necessary infrastructure, rock salt caverns appear to be a suitable solution for short-term storage. Metallic materials, especially those with a face-centered cubic (fcc) crystal structure, are susceptible to hydrogen-related degradation processes known as hydrogen embrittlement. The mechanisms of hydrogen embrittlement, which are still under discussion, manifest themselves, among other things, in a reduction in load-bearing capacity as well as in premature brittle failure at lower loads. This “vulnerability” is partly explained by the size of the interstitial defects in fcc structures, which might be exploited as pathways by hydrogen atoms (Campari et al., 2023). Rock salt has an fcc-crystal structure and, as an ionic crystal, could theoretically be susceptible to hydrogen embrittlement. To test this hypothesis, triaxial compressive strength tests are being carried out on a large-scale test rig. This study examines drill cores of coarse-grained rock salt (70 mm diameter) and synthetic samples with high porosity (~10 %). The latter are produced by compacting dry, coarse-grained salt with 60 to 260 kN over 1 to 28 days. A series of experiments was conducted at various strain rates (10^{-5} to 10^{-2} s⁻¹), confining pressures (from 0.5 to 10 MPa) and temperatures (from 20 to 60°C) to explore the brittle-ductile transition in rock salt and obtain comparative values for untreated material. The mechanical response of rock salt varies considerably with changes in these conditions: from fully ductile behavior at strains of up to 29 % to brittle failure after 2 % strain. The deformation mechanisms will be characterized using structural analysis. Future tests with hydrogen-containing samples will allow to explore the influence of hydrogen on the brittle-ductile transition as well as on the operating deformation mechanisms in rocks salt.

References

Campari, A., Ustolin, F., Alvaro, A., & Paltrinieri, N. (2023). A review on hydrogen embrittlement and risk-based inspection of hydrogen technologies. *international journal of hydrogen energy*, 48(90), 35316-35346.

Structural field observations of the Rechnitz Window (Austria, Hungary)

Bettine Sievers¹, Greta Siewert¹, Amina Redzematovic¹, Paola Manzotti², László Fodor^{3,4},
Benjamin Huet⁵, and Jan Pleuger¹

¹ *Institute of Geological Sciences, Freie Universität Berlin, bettine.sievers@fu-berlin.de*

² *Institute of Geological Sciences, Stockholm University*

³ *HUN-REN Institute of Earth Physics and Space Science, Sopron*

⁴ *Eötvös University Institute of Geography and Earth Sciences, Department of Geology, Budapest,*

⁵ *Geosphere Austria, Vienna*

The Rechnitz Window exposes Penninic rocks that are overlain by Austroalpine units and Neogene sediments in the easternmost part of the Eastern Alps. This region was strongly influenced by E–W extension and counterclockwise rotation in Miocene times (Mauritsch & Becke 1987). The large-scale structure of the Rechnitz Window is that of a metamorphic core complex bounded by a gently upwarped detachment zone (Tari 1996) and contains two tectonic units separated by a thrust. The upper unit is exposed to the west and the lower unit to the east.

Our study is based on field observations and structural analysis. The structures reveal four distinct ductile deformation events: (D1) a large-scale tight (sheath?) fold with an E–W elongation/fold axis, formed during a pre-extensional phase (prior to Miocene times); (D2) a penetrative mylonitic foliation and widespread isoclinal folds with axes parallel to a NE–SW trending stretching lineation. This lineation is associated with a top-to-the-northeast shear sense and probably related to an early extensional phase (Ratschbacher et al. 1990); (D3) localised top-to-the-east shear zones that are found mostly in the structurally highest part of the Rechnitz window; and (D4) E-vergent open to close folds overprinting the older structures. D1 and D2 structures were rotated during Miocene stages of deformation in a counterclockwise sense.

Assuming that D1 structures were formed prior to the Miocene rotation of about 30–45°, their original orientation would fit a top-to-the-northwest thrusting direction that is known from Penninic units elsewhere in the Alps. Likewise, D2 structures may have undergone a large amount of Miocene rotation such that the original direction of extension was west-east, fitting the overall direction of lateral extrusion of the Alps towards the Pannonian basin (Ratschbacher et al. 1991). D3 structures are probably still related to this extension but formed only after most of the counterclockwise rotation was already accomplished.

References

- Mauritsch, H.J. & Becke, M. (1987): Paleomagnetic investigation in the Eastern Alps and the southern border zone. In: Flügel, W. & Faupl, P. (eds): *Geodynamics of the Eastern Alps*. Deuticke, Vienna, 282–308.
- Ratschbacher, L., Frisch, W., Linzer, H.-G. & Merle, O. (1991): Lateral extrusion in the Eastern Alps, part 2: structural analysis. *Tectonics* 10, 257–271.
- Tari, G. (1996): Extreme crustal extension in the Rába river extensional corridor (Austria/Hungary). *Mitteilungen der Gesellschaft der Geologie- und Bergbaustudenten in Österreich* 41, 1–18.

Peak temperatures of metasediments from the Rechnitz Window Group (Austria, Hungary) determined by Raman spectroscopy on carbonaceous matter

Greta Siewert¹, Bettine Sievers¹, Amina Redzematovic¹, Paola Manzotti², Laszlo Fodor^{3,4}, Benjamin Huet⁵, and Jan Pleuger¹

¹ *Institute of Geological Sciences, Freie Universität Berlin, greta.siewert@fu-berlin.de*

² *Institute of Geological Sciences, Stockholm University*

³ *HUN-REN Institute of Earth Physics and Space Science, Sopron*

⁴ *Eötvös University Institute of Geography and Earth Sciences, Department of Geology, Budapest*

⁵ *Geosphere Austria, Vienna*

In the Rechnitz Window Group (Rechnitz, Bernstein, and Eisenberg windows) of the Eastern Alps, Penninic Units containing metasediments and metaophiolites are exposed below Austroalpine units. An upper and a lower unit can be distinguished in the Rechnitz Window. The upper unit contains blueschists that formed under conditions of 0.6–0.8 GPa/330–370 °C (qualitative estimate based on the blueschist's mineral paragenesis, Koller 1985). Assuming a rock density of 2700 kg/m³ and those pressures were lithostatic, this translates into a burial depth of ~ 20–28 km.

We determined metamorphic peak temperatures of 18 metasediment samples from the Rechnitz Window Group (Rechnitz, Bernstein, and Eisenberg windows) using Raman microspectroscopy on carbonaceous material in order to establish the peak metamorphic temperature pattern. Peak temperatures between 365 and 480 °C were determined for samples from both the upper and the lower Rechnitz unit. These temperatures are significantly higher than those reported for the peak-pressure stage. As no significant temperature difference can be detected between the lower and upper Rechnitz units, the temperature peak in both units was probably only reached after they were emplaced on top of each other. Higher peak temperatures of ≥ 450 °C are recorded in the southeast compared to ~ 400 °C in the northwest of the Rechnitz unit. The gradient can be interpreted as still roughly reflecting the dip direction of the subduction channel in which the units were buried and exhumed although Miocene counterclockwise rotation might have slightly modified the original orientation. However, the dip angle during the post-thrusting stage when peak temperatures were reached was probably rather small as estimated from temperature difference and (present-day) distance between the extremities. Therefore, we assume that the temperature peak was reached only after some amount of exhumation had occurred (i.e., to roughly 15–20 km depth assuming a vertical temperature gradient of ~ 25 °C/km).

References

Koller, F. (1985): Petrologie und Geochemie der Ophiolite des Penninikums am Alpenostrand. Jahrbuch der Geologischen Bundesanstalt 128, 83-150.

Progressive fabric development in crustal scale shear zone: insights from integrated AMS, PGR, and SPO analyses

Swagata Singha^{1*}, Tridib Kumar Mondal², Susanta Kumar Samanta¹,
and Subhabrata Das¹

¹Jadavpur University, Kolkata, India, swagatas2701@gmail.com

²Indian Statistical Institute, Kolkata, India

This study examines the development and spatial variation of deformational fabrics within the northeastern segment of the Singhbhum Shear Zone (SSZ), eastern India, using an integrated approach of Anisotropy of Magnetic Susceptibility (AMS), Point-Girdle-Random (PGR) fabric analysis, and Shape Preferred Orientation (SPO). A total of 120 oriented block samples were collected from seven distinct lithologies across the SSZ, yielding 674 oriented AMS specimens. AMS results reveal a consistent NW-SE-striking magnetic foliation and predominantly NE-trending magnetic lineation, broadly aligned with the field-measured shear fabrics across various lithologies. Mean magnetic susceptibility (K_m) ranges from negative to strongly positive values, reflecting mixed diamagnetic-paramagnetic mineralogy. The nonlinear relationship between K_m and degree of anisotropy (P_j) indicates dominant strain control on magnetic anisotropy. The predominance of oblate ellipsoids indicates that deformation is largely governed by flattening strains, while locally developed prolate fabrics mark zones of enhanced stretching. Magnetic fabrics are synchronous with the regional deformation, demonstrated by their alignment with shear-zone geometry and down-dip lineations.

PGR plots of magnetic lineation demonstrate systematic variation in magnetic fabric types, from weak or isotropic fabrics in lower-strain interior domains to well-developed tectonic and shear-related fabrics proximal to the shear zone. These patterns indicate progressive strain localization and lithology-dependent fabric evolution within the SSZ. SPO analysis of 10 oriented thin sections, analyzing over 18,000 mineral grains reveal variable angular relationships between mineral long axes and magnetic lineations, with stronger alignment and higher SPO intensity recorded near the shear zone. Together, the AMS-PGR-SPO dataset highlights that progressive deformation and lithology-controlled mineral fabrics jointly govern strain partitioning in ductile shear zones, providing a comprehensive framework for integrating magnetic and mineral fabrics in complex shear systems.

Ar-Ar geochronology II - Deciphering the code: Interpretation of complex Ar isotope data

Blanka Sperner¹ and Jörg A. Pfänder¹

¹ *Institut für Geologie, TU Bergakademie Freiberg, blanka.sperner@geo.tu-freiberg.de*

Owing to the continuous beta decay of ^{40}K to ^{40}Ar , argon isotope data from neutron-irradiated mineral separates or whole-rock splits released successively by step-heating experiments and measured by noble-gas mass spectrometry can be used in ideal cases to calculate an age for a rock. More precisely, what is observed is a cooling age for an individual mineral type, i.e., the time before present when a specific mineral type passed a distinct temperature (range) during cooling. In volcanic rocks due to fast cooling this can be easily attributed to the time of eruption, but in metamorphic rocks with multiple thermal overprints this diffusion-controlled phenomenon typically causes problems due to the loss or gain of radiogenic (and other) Ar. Therefore, newly grown or preexisting phases in metamorphic rocks such as micas, amphiboles or feldspars with comparatively low cooling temperatures, which are in the range of viable metamorphic reactions ($\sim 300\text{-}550^\circ\text{C}$) often provide complex Ar isotope data that are difficult to interpret and which do not necessarily result in any meaningful age. Here we present the results of a theoretical investigation of various scenarios of diffusion-controlled release of distinct argon components from a sample and evaluate the consequences on the resulting data set if presented in classical age spectra vs. three-isotope (isochron) plots. The modelled data were compared to real samples and help to better understand and read what is commonly termed 'complex data' or 'complex age spectra'. A very general conclusion of our investigation is that the classical and easy-to-read age spectrum plot is misleading in many cases, at least for samples that suffered a complex thermal history, whereas in distinct cases data complexity can be resolved in the three-Ar isotope space, leading to more robust age estimates and thus to – possibly – better constrained geological models.

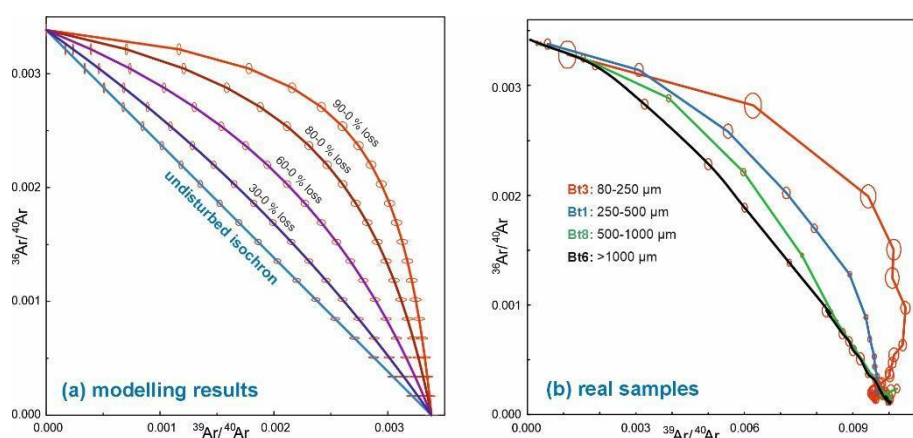


Figure 1: Examples of Ar-isotope data: (a) modelling results for grains containing gradual Ar loss, (b) results of step-heating experiments obtained from aliquots of a single sample but with different grain sizes. Loss increases with finer grain size due to increasing grain surface-to-volume ratio.

Marine Mn redox evolution tracks the Great Oxidation Event

Harilaos Tsikos^{1,2}, Jarryd Labuschagne³, Petros Koutsovitis², and Paul RD Mason⁴

¹ Martin Luther University of Halle-Wittenberg, Germany. htsikos@gmail.com

² University of Patras, Greece

³ Rhodes University, South Africa

⁴ Utrecht University, The Netherlands

Manganese-rich sedimentary rocks pre-dating the Great Oxidation Event (GOE) are scarce. Archean and Paleoproterozoic Iron Formations (IF) are occasionally enriched in bulk-rock Mn by a few wt% and have thus enjoyed intensive research in the context of the coevolution of oxygen and life in deep time [1,2]. Interpretations suggest transiently fully oxic marine conditions across the ambient water column during IF deposition, capable of oxidizing aqueous Mn(II) to insoluble Mn(IV) oxides in the presence of photosynthetic O₂. Molybdenum isotope ratios combined with low- $\delta^{13}\text{C}$ carbonates have been used as records of such processes through anaerobic diagenesis. However, positive Ce anomalies offering support for aerobic Mn(II) oxidation to Mn(IV) are lacking. This also applies to the giant IF-hosted Mn deposits of the 2.4Ga Hotazel Formation [3]. Here, aerobic oxidation of Mn(II) to Mn(III) is thought to be the main driver for primary Mn deposition, implying little to no concomitant oxidation of Ce(III) to Ce(IV).

Unequivocal evidence for oxidation of Mn and Ce to their tetravalent states is preserved in a thin (~3m) Mn-rich horizon at the base of the ca. 2.3Ga Lephala black shale sequence of Botswana, a lateral equivalent to the syn-GOE Timeball Hill Formation in adjacent South Africa. The Mn-rich bed contains well-preserved, mm-scale micronodules that are texturally very similar to Mn nodules from the modern ocean floor. The Lephala Mn nodules are pseudomorphically preserved through replacement by low- $\delta^{13}\text{C}$ kutnahorite. Whole-rock geochemical analyses reveal clear positive Ce anomalies ($\text{Ce}/\text{Ce}^*=1.5\text{-}3$) in all samples, in support of a Ce(IV)-bearing, Mn(IV) precursor. Such signatures are replicated in several sedimentary Mn deposits across the entire Rhyacian period. We conclude that the Lephala Mn nodules may record the emergence of Mn oxidizing bacteria capable of driving complete oxidation of Mn(II) to Mn(IV) for the first time at the dawn of the GOE.

References

- [1] Planavsky et al., 2014. *Nat. Geosci.* 7, 283-286.
- [2] Kurzwil et al., 2016. *Earth Planet. Sci. Lett.* 452, 69-78.
- [3] Mhlanga et al., 2022. *Earth-Sci. Rev.*, 104759.

An isoclinal and boudinaged synformal anticline in the Reckner Nappe of the Tarntal Mesozoic (Lower Austroalpine), Eastern Alps

Kamil Ustaszewski¹ and Philipp Balling¹

¹ Friedrich-Schiller Universität Jena, Institut für Geowissenschaften. kamil.u@uni-jena.de

The Tarntal Mesozoic in the Tux Alps in Tirol, Austria, forms a tectonic unit hosting a Mesozoic rifted passive margin succession at the NW margin of the Tauern Window. At large, this unit occupies a tectonic position within the Lower Austroalpine units, between the structurally overlying Upper Austroalpine Innsbruck Quartzphyllite Unit and underlying Penninic units (Fig. 1). Internally, it comprises three sub-units. These are, from top to bottom, (i) the structurally highest Reckner Complex with evidence for Paleogene blueschist-facies overprint (Dingeldey et al., 1997), (ii) the intermediate Reckner Nappe and (iii) the lowermost Hippold Nappe (Enzenberg-Praehauser, 1976). All sub-units provide evidence for extensional overprint preceding Alpine shortening, including Lower Jurassic isotopic ages in the Reckner Complex reflecting seafloor metamorphism of tectonically exhumed mantle (Ratschbacher et al., 2004), as well as large volumes of Lower to Middle Jurassic synrift-breccia in the Reckner and Hippold nappes. Geological mapping in the area suggests that the Reckner Nappe, exposed for c. 3 km perpendicular to its strike, forms a north-vergent isoclinal anticline with discontinuous slivers of Norian Hauptdolomit in its core, which likely form boudins resulting from N-S-stretching during Alpine subduction and subsequent exhumation. The local overprint into a synformal anticline resulted from N-S-convergence postdating nappe stacking. We think that the area was affected by at least three phases of thrusting (D0, D1 and D2), with D2 forming an out-of-sequence thrust creating a sandwich geometry where the Tarntal Mesozoic both overlies and underlies the Innsbruck Quartzphyllite Unit (Fig. 1).

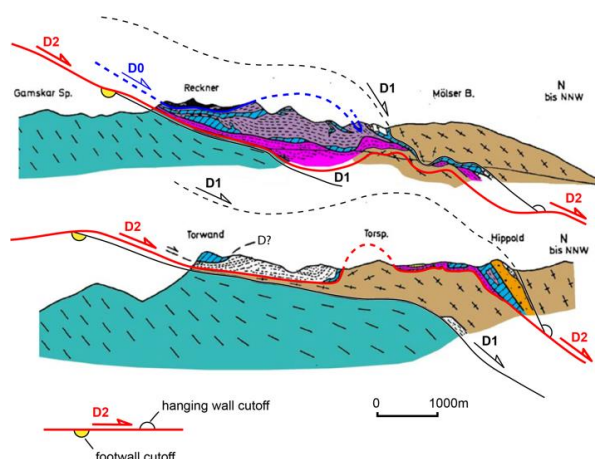


Figure 1: Reinterpretation of cross sections of Thiele (1976) in terms of a polyphase tectonic development with three thrusting phases D0, D1 and D2, resulting in the currently observed sandwich position of the Tarntal Mesozoic with both underlying and overlying Quartz Phyllite Unit (brown).

References

- Dingeldey, C., et al. (1997): "P -T-t history of the Lower Austroalpine Nappe Complex in the "Tarntaler Berge" NW of the Tauern Window: implications for the geotectonic evolution of the central Eastern Alps." *Contributions to Mineralogy and Petrology* 129: 1-19.
- Enzenberg-Praehauser, M. (1976). "Zur Geologie der Tarntaler Breccie und ihrer Umgebung im Kamm Hippold-Kalkwand (Tuxer Voralpen, Tirol)." *Mitt. Ges. Geol. Bergbaustud. Österr.* 23: 163-180.
- Ratschbacher, L., et al. (2004). "Formation, subduction, and exhumation of Penninic oceanic crust in the Eastern Alps: time constraints from ⁴⁰Ar/³⁹Ar geochronology." *Tectonophysics* 394: 155-170.
- Thiele, O. (1976). "Der Nordrand des Tauernfensters zwischen Mayrhofen und Inner Schmirn (Tirol)." *Geologische Rundschau* 65: 410-421.

Two types of serpentinite from the Saxon Granulite Massif (Bohemian Massif, Germany)

Sebastian Weber¹, Martin Keseberg², and Thorsten Nagel²

¹ Saxon State Agency for Environment, Agriculture and Geology, 09599 Freiberg, Halsbrücker Str. 31a, Germany

²Institut für Geologie, TU Bergakademie Freiberg, Bernhard-von-Cotta-Straße 2, 09599 Freiberg, Germany

The north-western margin of the Bohemian Massif hosts numerous high-grade metamorphic rocks that occur in the Erzgebirge and the Granulite Massif, exhibiting a complex geodynamic evolution (Rötzler & Timmerman, 2020). They are members of a continental subduction zone system that developed along the northern plate boundary of Gondwana during the Variscan orogeny between 390 and 340 Ma (Kotková et al., 2025). These high-grade felsic rocks, which have undergone intense high-pressure metamorphic conditions, frequently contain ultramafic bodies that are serpentinitized to varying degrees. In domains where serpentinitization has not completely replaced the mineralogy of the protolith, remnants of the peridotitic mantle rock can be studied. In the Erzgebirge and Granulite Massif, these ultramafic pods often comprise macroscopically visible, cm-sized garnet blasts in association with orthopyroxene + clinopyroxene and olivine. This mineral assemblage is considered to originate from a spinel-bearing protolith. The maximum metamorphic conditions for the garnet-bearing ultramafic bodies were determined to be distinct for the Erzgebirge at 900 °C and 30-35 kbar and for the Granulite Mountains at 1300-1400 °C and 32 kbar (Schmädicke and Evans, 1997; Schmädicke et al. 2010). Both units reflect fundamentally different exhumation histories, which in turn resulted in the formation of distinct retrograde reaction textures. In addition to these prominent garnet-bearing ultramafic bodies, a second type of peridotite exhibiting garnet exsolution textures in pyroxene is also found in the Granulite Massif (Schmädicke et al. 2010). Garnet exsolution textures display a fundamentally different chemistry than the cm-sized garnet grains. This contribution deals with the petrological significance of these garnet exsolution textures in this type of peridotite in the overall context of regional geological development.

References

- Kotková J., Čopjaková, R., Kubeš, M., Ackerman L., Sláma, J., Schmädicke, E., Holá, M. (2025) Melting and metasomatic history of the lithospheric mantle in the Erzgebirge UHP terrane: Constraints from trace elements, Sr–Nd–Hf–Os isotopes and Lu–Hf dating. *Lithos*, 516–517, 108234.
- Schmädicke, E., Evans, B.W. (1997) Garnet-bearing ultramafic rocks from the Erzgebirge, and their relation to other settings in the Bohemian Massif. *Contrib Mineral Petrol*, 127, 57–74.
- Schmädicke, E., Gose J., Will, T.M. (2010) The P–T evolution of ultra high temperature garnet-bearing ultramafic rocks from the Saxonian Granulitgebirge Core Complex, Bohemian Massif, *J. metamorphic Geol.*, 28, 489–508.
- Rötzler, J., Timmerman, M.J. (2020). Geochronological and petrological constraints from the evolution in the Saxon Granulite Massif, Germany, on the Variscan continental collision orogeny. *Journal of Metamorphic Geology*, 39, 3-38. 10.1111/jmg.12559

Multistage vein fracturing and gold mineralization: insights from the Linglong orogenic gold deposit, China

Peng-Cong Zhang^{1,2}, Anna Rogowitz¹, Hao-Cheng Yu², Clifford Patten³,
and Kun-Feng Qiu²

¹ *University of Innsbruck, Department of Geology Pengcong.Zhang@student.uibk.ac.at*

² *China University of Geosciences, Beijing, School of Earth Sciences and Resources*

³ *University of Innsbruck, Department of Mineralogy and Petrography*

Orogenic gold deposits record multiple crack seal cycles in auriferous quartz veins, yet the fundamental mechanisms governing repeated fracturing and its linkage to gold mineralization remain poorly constrained. This study focuses on auriferous quartz veins from the Linglong gold deposit, China, integrating petrography, structural analysis, electron probe microanalysis element mapping, and electron backscatter diffraction (EBSD) analysis to constrain the mechanical processes driving recurrent fracturing and gold precipitation.

Six distinct vein generations are identified based on crosscutting relationships and are termed Vein 1 to Vein 6. Vein 2 and Vein 3 represent the principal gold mineralizing stage and display a consistent assemblage of visible gold, pyrite, pyrrhotite, galena, sphalerite, quartz, and dolomite. Vein 2 exhibits well developed synthetic shear band geometries, recording top to the SW shearing. Veining event 3 is characterized by arrays of extensional microcracks subparallel to Vein 2, indicating formation under the same stress regime. Element mapping demonstrates that pyrite (Py2) from Vein 2 was fractured during the Vein 3 event and subsequently resealed by newly precipitated pyrite (Py3) and base metal sulfides. EBSD analysis reveals that Py3 exhibits crystallographic orientations distinct from those of the host Py2 where open space existed, indicating new nucleation during fluid infiltration, whereas in narrow microfractures the new pyrite inherits the crystallographic orientation of the host, suggesting epitaxial overgrowth under spatially restricted conditions. Recurrent vein formation reflects episodic fracturing that created transient permeability, resulting in repeated pressure drops and associated gold deposition. Furthermore, deformation induced fluid and diffusion pathways (i.e., fractures and dislocation networks) in Py2 result in local remobilization of As. Collectively, these results demonstrate that even within a uniform tectonic regime, repeated vein reactivation can be expressed through distinct mechanical processes. Fracture generated fluid pathways sustain hydrothermal circulation and govern the localization and accumulation of gold in orogenic systems.